ICI Mitigation Schemes for Uncoded OFDM over Channels with Doppler Spreads and Frequency Offsets – Part II: Asymptotic Analysis

Takeshi Hashimoto, Abdullah S. Alaraimi, and Chenggao Han
Graduate School of Informatics and Engineering, the University of Electro-Communications, Chofu, Tokyo 182-8585, Japan
Email: {hasimoto, hana}@ee.uec.ac.jp

***Abstract*— In the second part of this two-part paper, we derive approximations to the signal-to-interference plus noise power ratio (SINR) attainable by PCC, SCC, and windowing and compare their performances in terms of SINR. We also derive an asymptotically optimal window and discuss the optimality of the triangular window for ICI reduction. Finally, we derive approximations to bit-error-rate (BER) attainable by SCC and cyclic cancellation coding (CCC) when optimal combining is used at the receiver and compare these approximations with simulation results. We also discuss the relationships between these ICI mitigation schemes and other transmission schemes.**

I. Introduction

The Doppler (frequency) spread and carrier frequency offset (CFO) cause intercarrier interference (ICI) in an orthogonal frequency-division multiplexing (OFDM) system and severely affects the bit-error-rate (BER) behavior of the system. Thus, there have been proposed many ICI suppression schemes, among which Nyquist windowing, polynomial cancellation coding (PCC), and symmetric cancellation coding (SCC) are simple and yet effective schemes. In the first part of this two-part paper, we reviewed those schemes and discussed some of known results between them.

In this second part of the two-part paper, we derive approximations to the signal-to-interference plus noise power ratio (SINR) and BER expressions for PCC, SCC, and receiver windowing applied to uncoded OFDM systems. Especially, we derive the optimal window for receiver windowing that minimizes SINR under the condition that the Doppler spread and CFO are sufficiently small. The optimal window is a double jump Nyquist window and approaches to the triangular window as the large signal-to-noise power ratio (SNR) decreases. This result supports the observations in [1] and in [2]. Based on the derived SINR approximations, we compare these schemes in terms of SINR and BER. In the last half of this part, we derive BER approximations for the diversity schemes, SCC and CCC, and compare with PCC and windowing in terms of BER. The results reveal the effectiveness of the diversity schemes compared to the self-ICI-cancellation schemes, which has not been fully recognized.

In the followings, all the references preceded by "I-" are those found in the first Part.

The rest of this second part of the two-part paper is organized as follows. In Section II, we prepare some preliminaries and, in Section III, we calculate SINR approximations for the respective self-ICI-cancellation and windowing schemes and compare their performances. In Section IV, we consider two diversity schemes for ICI mitigation and give BER approximations. Section V is the conclusion.

II. Preliminaries

We consider OFDM-based signals of symbol period T (sec) $\{x_k\}$ sampled in sampling period $T_\mathrm{s} = \frac{T}{N}$, where N is the number of subcarriers and is assumed to be an even integer.

The channel is a discrete-time, time-variant multipath Rayleigh fading channel

$$y_k = \sum_{\ell=0}^{L-1} h_{k,\ell} x_{k-\ell} + w_k,$$

where w_k is the discrete-time, complex-valued white Gaussian noise with variance $\sigma_\mathrm{n}^2 = NN_o$. We suppose $L-1 \le N_\mathrm{G}$.

We assume the wide-sense stationary and uncorrelated scattering (WSSUS) model for the fading processes [3], [4], [5]. In practice, however, there is a CFO between the transmitter and receiver local oscillators, and we assume that the channel coefficients $h_{k,\ell}$ are circularly symmetric (CS) Gaussian random processes [6] satisfying

$$\mathrm{E}[h_{k,\ell} h^*_{k',\ell'}] = p_\ell e^{j\omega_O T_s[k-k']} J_0(\omega_D T_s[k-k'])\delta_{\ell-\ell'}, \quad (1)$$

where p_ℓ is the power of the ℓth path, $\omega_D \triangleq 2\pi f_D$ (rad/sec) is the (maximum) Doppler frequency, $\omega_O \triangleq 2\pi f_O$ (rad/sec) is the CFO, $J_0(x)$ is the zeroth-order Bessel function of the first kind, and δ_k is Kronecker's delta function. Without loss of generality, we assume $\sum_{\ell=0}^{L-1} p_\ell = 1$.

Under the presence of ICI, the received signal, after DFT and appropriate processing, is generally expressed as

$$R(n) = A(n)a_n + I(n) + W(n)$$

doi:10.4304/jcm.7.9.686-700

where a_n is the transmitted data symbol, $A(n)$ is its complex amplitude, $I(n)$ is the ICI term, and $W(n)$ is the noise term. If a_n are mutually independent random variables with zero mean and variance $\mathrm{E}\left[|a_n|^2\right] = E_\mathrm{s}$, then SINR is given as

$$\Gamma(n) = \frac{E_\mathrm{s} \cdot \mathrm{E}\left[|A(n)|^2\right]}{\mathrm{E}\left[|I(n)|^2\right] + \mathrm{E}\left[|W(n)|^2\right]}.$$

We employ, in the following discussions, the Gaussian interference assumption that the interference $I(n)$ is well approximated by a CS Gaussian random variable independent of $A(n)$. Moreover, different schemes are compared on the basis of the fixed total transmit power for the same bandwidth.

We let

$$\alpha_k \triangleq e^{j\omega_O T_s k} J_0(\omega_D T_s k)$$

and let its power spectrum density (PSD) be (see Appendix I) $\mathcal{A}(\omega) \triangleq \sum_{k=-\infty}^{\infty} \alpha_k e^{-j\omega k}$. Moreover, under the convention $\mathcal{A}_n(\omega) \triangleq \frac{1}{n}\mathcal{A}\left(\frac{\omega}{n}\right)$, let us introduce spectral moments

$$\mathcal{S}_\ell \triangleq \frac{1}{2\pi} \int \omega^\ell \mathcal{A}_N(\omega)\, d\omega. \quad (2)$$

It is not difficult to show $\mathcal{S}_2 = (\omega_O T)^2 + \frac{1}{2}(\omega_D T)^2$ and $\mathcal{S}_4 = (\omega_O T)^4 + 3(\omega_O T)^2(\omega_D T)^2 + \frac{3}{8}(\omega_D T)^4$. In the following discussions, we assume[1]

$$\frac{\mathcal{S}_1}{N^2},\ \frac{\mathcal{S}_2}{N},\ \mathcal{S}_i\ (4 \le i) \text{ are negligible compared to } \mathcal{S}_2. \quad (3)$$

We also introduce the following spectral functions

$$P_a \triangleq \sum_{\ell=0}^{L-1} p_\ell e^{-j\frac{2\pi a \ell}{N}}, \quad (4)$$

$$F_a \triangleq \frac{1}{N} \sum_{k=-\frac{N}{2}+1}^{\frac{N}{2}-1} \alpha_{2k} e^{-j\frac{2\pi a k}{N}}, \quad (5)$$

$$F_{a,b} \triangleq \frac{1}{N^2} \sum_{k=0}^{N-1} \sum_{k'=0}^{N-1} \alpha_{k-k'} e^{-j\frac{2\pi a k}{N}} e^{j\frac{2\pi b k'}{N}}.$$

We note that $P_a^* = P_{-a}$, $F_a^* = F_{-a}$, and $F_{a,b}^* = F_{b,a}$.

Finally, for integers a and b, we let $[a]_b \triangleq a \bmod b$.

III. Asymptotic analysis of PCC, SCC, and windowing

A. Normal OFDM

In the first part, it is shown that

$$W(n) = \frac{1}{N} \sum_{k=0}^{N-1} w_k e^{-j\frac{2\pi n k}{N}} \quad (6)$$

and, for

$$A_{m,n} = \frac{1}{N} \sum_{k=0}^{N-1} \sum_{\ell=0}^{L-1} h_{k,\ell} e^{j\frac{2\pi(m-n)k}{N}} e^{-j\frac{2\pi m \ell}{N}}, \quad (7)$$

that

$$A(n) = A_{n,n} \text{ and } I(n) = \sum_{m \ne n} a_m A_{m,n}.$$

From the WSSUS assumption (1), the power of $A_{m,n}$ given in (7) is calculated as

$$\mathrm{E}\left[|A_{m,n}|^2\right] = F_{n-m,n-m}.$$

Then, the power of the signal coefficient is

$$\mathrm{E}\left[|A(n)|^2\right] = F_{0,0}.$$

According to $\sum_{m=0}^{N-1} e^{j\frac{2\pi m k}{N}} = N\delta_{[k]_N}$ and $\alpha_0 = 1$, we can show $\sum_{m=0}^{N-1} \mathrm{E}\left[|A_{m,n}|^2\right] = 1$. Thus, the interference power is given by

$$\begin{aligned}\mathrm{E}\left[|I(n)|^2\right] &= \sum_{m=0}^{N-1} \mathrm{E}\left[|A_{m,n}|^2\right] - \mathrm{E}\left[|A(n)|^2\right] \\ &= E_\mathrm{s}\left(1 - F_{0,0}\right).\end{aligned}$$

The noise power is $\mathrm{E}\left[|W_n|^2\right] = N_o$. Thus, if we let the signal-to-noise ratio (SNR) $\bar{\gamma} \triangleq \frac{E_\mathrm{s}}{N_o}$, then the SINR of the normal OFDM is given as

$$\Gamma^\mathrm{N}(n) = \frac{F_{0,0}}{1 - F_{0,0} + \bar{\gamma}^{-1}} \approx \left\{\frac{\mathcal{S}_2}{12} + \frac{1}{\bar{\gamma}}\right\}^{-1}, \quad (8)$$

where the last approximation follows from Lemma A1 in Appendix I and Assumption (3). This approximation agrees with those in [7] and [8].

B. PCC-OFDM

In the first part, it is shown that, for W_n given in (6),

$$W^\mathrm{P}(n) = \frac{1}{\sqrt{2}} W_{2n} - \frac{1}{\sqrt{2}} W_{2n+1}$$

and, for

$$\begin{aligned}A^\mathrm{P}_{m,n} &= \frac{1}{2}\left(A_{2m,2n} - A_{2m+1,2n}\right) \\ &\quad - \frac{1}{2}\left(A_{2m,2n+1} - A_{2m+1,2n+1}\right),\end{aligned}$$

that

$$A^\mathrm{P}(n) = A^\mathrm{P}_{n,n} \text{ and } I^\mathrm{P}(n) = \sum_{\substack{m=0 \\ m \ne n}}^{\frac{N}{2}-1} a'_m A^\mathrm{P}_{m,n}.$$

Thus, the power of the signal coefficient is calculated as

$$\begin{aligned}&\mathrm{E}\left[|A^\mathrm{P}(n)|^2\right] \\ &= \frac{1}{4N^2} \sum_{\ell=0}^{L-1} p_\ell \sum_{k=0}^{N-1} \sum_{k'=0}^{N-1} \alpha_{k-k'} \left\{1 - e^{j\frac{2\pi(k-\ell)}{N}}\right\} \\ &\quad \times \left\{1 - e^{-j\frac{2\pi k}{N}}\right\} \left\{1 - e^{-j\frac{2\pi(k'-\ell)}{N}}\right\} \left\{1 - e^{j\frac{2\pi k'}{N}}\right\} \\ &= \frac{1 + \Re[P_1]}{2} F_{0,0} + \frac{1}{2} F_{1,1} \\ &\quad + \frac{1}{2} \Re\left[P_{-1} F_{1,-1} - (1 + P_{-1})(F_{1,0} + F_{0,-1})\right].\end{aligned}$$

[1]We can not specify how large (or small) N (or $\mathcal{S}_i$) should be since derivations are complex, but can only claim it should be sufficiently large (or small).

On the other hand, the sum of all the powers of coefficients is calculated, from the identity $\sum_{m=0}^{\frac{N}{2}-1} e^{-j\frac{4\pi(k-k')(n-m)}{N}} = \frac{N}{2}\delta_{[k-k']_{N/2}}$, as

$$\begin{aligned}\sum_{m=0}^{\frac{N}{2}-1} \mathrm{E}\left[|A^{\mathrm{P}}_{m,n}|^2\right] &= \sum_{m=0}^{\frac{N}{2}-1} \frac{1}{4N^2} \sum_{\ell=0}^{L-1} p_\ell \sum_{k=0}^{N-1}\sum_{k'=0}^{N-1} \alpha_{k-k'} \left\{1-e^{j\frac{2\pi(k-\ell)}{N}}\right\} \\ &\quad \times \left\{1-e^{-j\frac{2\pi k}{N}}\right\}\left\{1-e^{-j\frac{2\pi(k'-\ell)}{N}}\right\}\left\{1-e^{j\frac{2\pi k'}{N}}\right\} \\ &\quad \times e^{-j\frac{4\pi(n-m)(k-k')}{N}} \\ &= \frac{1}{2}+\frac{1}{4}\Re[P_1]+\frac{1}{4}\Re[P_1]\cdot\Re[\alpha_{\frac{N}{2}}].\end{aligned}$$

We assume that[2]

$$P_{\pm 1} \approx 1 \qquad \text{and} \qquad N\sin\frac{\pi}{N} \approx \pi. \tag{9}$$

Then, applying Lemma A1 in Appendix I to (9), we have

$$\mathrm{E}\left[|A^{\mathrm{P}}(n)|^2\right] \approx F_{0,0}+\frac{\mathcal{S}_2}{2N^2\sin^2\frac{\pi}{N}} \approx 1-\left(\frac{1}{6}-\frac{1}{\pi^2}\right)\frac{\mathcal{S}_2}{2}.$$

On the other hand, from the approximation (31) in Appendix I and assumption (9), we have

$$\sum_{m=0}^{\frac{N}{2}-1} \mathrm{E}\left[|A^{\mathrm{P}}_{m,n}|^2\right] \approx 1-\frac{\mathcal{S}_2}{32}.$$

Thus, the interference power is approximated as

$$\mathrm{E}\left[|I^{\mathrm{P}}(n)|^2\right] \approx E'_{\mathrm{s}}\left(\frac{5}{48}-\frac{1}{\pi^2}\right)\frac{\mathcal{S}_2}{2}$$

The noise power is $\mathrm{E}\left[|W^{\mathrm{P}}(n)|^2\right] = N_o$.

Thus, the SINR is approximated as

$$\Gamma^{\mathrm{P}}(n) \approx \left\{\left(\frac{5}{48}-\frac{1}{\pi^2}\right)\frac{\mathcal{S}_2}{2}+\frac{1}{2\bar{\gamma}}\right\}^{-1}, \tag{10}$$

where we let $E'_{\mathrm{s}} = 2E_{\mathrm{s}}$.

C. SCC-OFDM

For SCC, we first consider a flat fading channel ($L = 1$) and subtraction combining with $\phi_n^{(1)} = -\phi_n^{(2)} = \frac{1}{\sqrt{2}}$. For a frequency-selective fading channel, only the result is given for the subtraction combining later since the result is not promising in spite of complicated analysis.

In the first part, it is shown that

$$W^{\mathrm{S}}(n) = \phi_n^{(1)}W_n + \phi_n^{(2)}W_{N-1-n}$$

and, for

$$\begin{aligned}A^{\mathrm{S}}_{m,n} &= \phi_n^{(1)}(A_{m,n}-A_{-1-m,n}) \\ &\quad +\phi_n^{(2)}(A_{m,-1-n}-A_{-1-m,-1-n}),\end{aligned}$$

[2]For a relatively small delay spread, the first approximation hold as seen in Fig. 8, while the second approximation holds for N larger than several tens.

that

$$A^{\mathrm{S}}(n) = A^{\mathrm{S}}_{n,n} \quad \text{and} \quad I^{\mathrm{S}}(n) = \sum_{\substack{m=0 \\ m\neq n}}^{N-1} a'_m A^{\mathrm{S}}_{m,n}$$

Thus, the power of the signal coefficient is calculated as

$$\begin{aligned}&\mathrm{E}\left[|A^{\mathrm{S}}(n)|^2\right] \\ &= \frac{1}{4N^2}\sum_{k=0}^{N-1}\sum_{k'=0}^{N-1}\alpha_{k-k'}\left|e^{j\frac{2\pi nk}{N}}-e^{-j\frac{2\pi(n+1)k}{N}}\right|^2 \\ &\qquad \times\left|e^{-j\frac{2\pi nk'}{N}}-e^{j\frac{2\pi(n+1)k'}{N}}\right|^2 \\ &= F_{0,0}+\frac{1}{2}F_{2n+1,2n+1}+\frac{1}{2}\Re\big[F_{2n+1,-(2n+1)} \\ &\qquad -2F_{2n+1,0}-2F_{0,-(2n+1)}\big].\end{aligned} \tag{11}$$

On the other hand, from the identity

$$\begin{aligned}&\sum_{m=0}^{\frac{N}{2}-1}\left\{e^{j\frac{2\pi mk}{N}}-e^{-j\frac{2\pi(m+1)k}{N}}\right\}\left\{e^{-j\frac{2\pi mk'}{N}}-e^{j\frac{2\pi(m+1)k'}{N}}\right\} \\ &\quad = N\delta_{[k-k']_N}-Ne^{-j\frac{2\pi k}{N}}\delta_{[k+k']_N},\end{aligned}$$

we have

$$\begin{aligned}&\sum_{m=0}^{\frac{N}{2}-1}\mathrm{E}\left[|A^{\mathrm{S}}_{m,n}|^2\right] \\ &= \frac{1}{4N^2}\sum_{m=0}^{\frac{N}{2}-1}\sum_{k=0}^{N-1}\sum_{k'=0}^{N-1}\alpha_{k-k'} \\ &\quad \times\left\{e^{j\frac{2\pi mk}{N}}-e^{-j\frac{2\pi(m+1)k}{N}}\right\}\left\{e^{-j\frac{2\pi mk'}{N}}-e^{j\frac{2\pi(m+1)k'}{N}}\right\} \\ &\quad \times\left\{e^{-j\frac{2\pi nk}{N}}-e^{j\frac{2\pi(n+1)k}{N}}\right\}\left\{e^{j\frac{2\pi nk'}{N}}-e^{-j\frac{2\pi(n+1)k'}{N}}\right\} \\ &= \frac{1}{2}+\frac{1}{4N}\sum_{k=-\frac{N}{2}+1}^{\frac{N}{2}-1}\alpha_{2k}\left\{e^{-j\frac{2\pi(2n+1)k}{N}}+e^{j\frac{2\pi(2n+1)k}{N}}+2\right\} \\ &= \frac{1}{2}(1+F_0)+\frac{1}{2}\Re\left[F_{2n+1}\right],\end{aligned} \tag{12}$$

where, in the second equality, we used $\sum_{k=0}^{N-1} e^{j\frac{2\pi(2n+1)k}{N}} = 0$ for all n and the change of parameters, $k-\frac{N}{2} \to k$.

Applying Lemma A1 in Appendix I to (11), we have an approximation $\mathrm{E}\left[|A^{\mathrm{S}}(n)|^2\right] \approx 1$. On the other hand, from (11) and (12), the interference power is approximated as

$$\begin{aligned}&\mathrm{E}\left[|I^{\mathrm{S}}(n)|^2\right] \\ &= \frac{E'_{\mathrm{s}}}{2}(1+F_0)+\frac{E'_{\mathrm{s}}}{2}\Re\left[F_{2n+1}\right]-E'_{\mathrm{s}}F_{0,0} \\ &\quad -\frac{E'_{\mathrm{s}}}{2}F_{2n+1,2n+1} \\ &\quad -\frac{E'_{\mathrm{s}}}{2}\Re\big[F_{2n+1,-(2n+1)}-2F_{2n+1,0}-2F_{0,-(2n+1)}\big] \\ &\approx -\frac{E'_{\mathrm{s}}\mathcal{S}_2}{12N^2}+\frac{E'_{\mathrm{s}}\mathcal{S}_4}{720}+\frac{E'_{\mathrm{s}}\mathcal{S}_2}{2N^2\sin^2\frac{\pi(2n+1)}{N}} \\ &\quad -\frac{E'_{\mathrm{s}}}{2}F_{2n+1,2n+1} \\ &\quad -\frac{E'_{\mathrm{s}}}{2}\Re\big[F_{2n+1,-(2n+1)}-2F_{2n+1,0}-2F_{0,-(2n+1)}\big]\end{aligned}$$

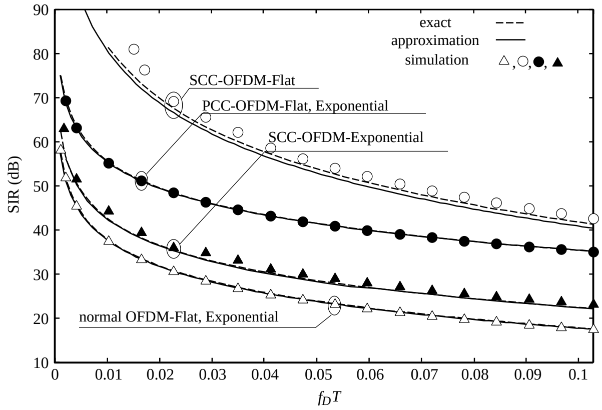

Figure 1. SIR comparison between the normal OFDM, PCC-OFDM, and SCC-OFDM for a multipath fading channel for $N = 1024$.

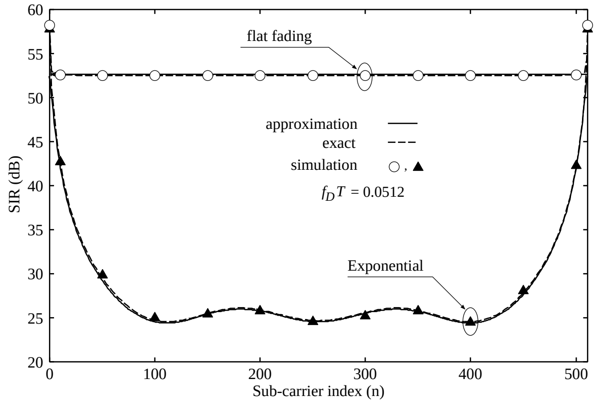

Figure 2. SIR profile of SCC-OFDM over the flat fading channel and the four-path fading channel, $N = 1024$.

$$\approx \frac{E_s' \mathcal{S}_4}{720} + \frac{E_s' \mathcal{S}_2}{6N^2}, \tag{13}$$

where the first approximation comes from Lemma A1 and Lemma A2 in Appendix I and the second approximation is shown in Appendix II. The noise power is $\mathrm{E}\left[|W^{\mathrm{S}}(n)|^2\right] = N_o$.

Therefore, the SINR is given by

$$\Gamma^{\mathrm{S}}(n) \approx \left\{ \frac{\mathcal{S}_4}{720} + \frac{1}{2\bar{\gamma}} \right\}^{-1}$$

where we let $E_s' = 2E_s$. This indicates that SCC-OFDM shows a performance superior to PCC-OFDM over the flat fading channel.

For a frequency-selective fading channel, we can show, for $\frac{1}{N} \ll 1 - \Re[P_{2n+1}]$ and $\mathcal{S}_4 \ll \mathcal{S}_2$, the approximation

$$\Gamma^{\mathrm{S}}(n) \approx \frac{(1 + \Re[P_{2n+1}])\, F_{0,0}}{1 - F_0 + \frac{1}{\bar{\gamma}} + (1 + \Re[P_{2n+1}])\,(F_0 - F_{0,0})}$$
$$\approx \frac{\frac{1}{2}\,(1 + \Re[P_{2n+1}])\left(1 - \frac{\mathcal{S}_2}{12}\right)}{(1 - \Re[P_{2n+1}])\left(\frac{\mathcal{S}_2}{24} - \frac{\mathcal{S}_4}{360}\right) + \frac{\mathcal{S}_4}{720} + \frac{1}{2\bar{\gamma}}} \tag{14}$$

If $1 - \Re[P_{2n+1}]$ and $\frac{1}{2}\,(1 + \Re[P_{2n+1}])$ are comparable to one, which is the case in general, the the above SINR is better by only several dBs than the SINR (8) of the normal OFDM, which is observed also in simulation. The derivation of the above SINR expression is, however, omitted in this paper since the result is not very much encouraging.

D. Preliminary comparisons

Before proceeding further, we compare the exact calculations, approximations obtained above, and simulation results.

In Fig. 1, we show the signal-to-interference ratio (SIR), the SINR for SNR $= \infty$, of the normal OFDM, PCC-OFDM, and SCC-OFDM with $N = 1024$ over a four-path fading channel with power-delay profile (PDP) $\{p_\ell\} = \{0.342, 0.271, 0.216, 0.171\}$, which is a truncated and normalized exponential PDP with the root-mean-square (RMS) delay spread approximately T_s. In the figure, the approximations are shown in solid lines and the exact values calculated from the original ICI expressions are shown in broken lines, while the simulation values are plotted in marks. In the case of SCC-OFDM, SIR shown in the figure is the average over all the subcarriers except for the respective 20 subcarriers in the extreme sides, and the exact and simulation values for the flat fading channel are calculated in the same manner while the approximation values are the approximations at the center subcarrier, namely, $n = 250$. In the rage of $f_D T$ shown in the figure, the exact and approximated calculations for the normal OFDM, PCC-OFDM, and SCC-OFDM agree each other and agree with the simulation results except for SCC-OFDM. The small discrepancy between theory and simulation in SCC seems to be the effects of the SIR behaviors at the extreme sides.

In Fig. 2, we show the SIR profiles of SCC-OFDM as functions of subcarrier index for the same parameters as the previous figure. In the simulation, we used the sum-of-sinusoid algorithm [4] for fading process generation for all the cases and obtained the average interference power at each subcarrier position. The SIR profiles considerably vary at the both sides and this seems to explain the discrepancy found in Fig. 1. Thus, we may conclude that the approximation is almost exact in this range of $f_D T$.

In Fig. 3, we show the SIR of the normal OFDM, PCC-OFDM, and SCC-OFDM with $N = 1024$ over a single-path, constant frequency offset channel with $h_{k,0} = e^{j\frac{2\pi k f_O T}{N}}$. Since fading is not considered, the match between the exact calculation and simulation is quite well. In this figure, $f_O T$ is varied up to 0.5 and, as we can see, the exact calculations and approximations agree with each other up to $f_O T$ approximately 0.15. Since SIR is independent of the ICI distribution, this conclusion is considered to carry over for $f_D T$.

It is interesting to compare Fig. 3 and the result for DCT-OFDM, Fig. 4 in [9] since SCC-OFDM and DCT-OFDM are basically the same except for the inter-subcarrier space. In fact, if we change the scale of $f_O T$ for SCC-OFDM by moving the plot at $f_O T = 0.5$ to $f_O T = 0.25$, then we have Fig. 4 in [9]. Thus, our SINR

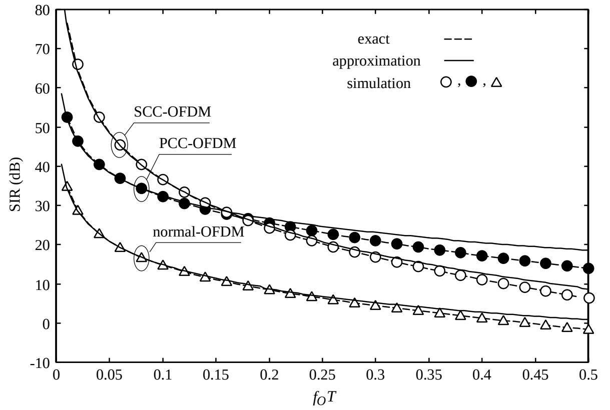

Figure 3. SIR comparison between the normal OFDM, PCC-OFDM, and SCC-OFDM over a constant frequency-offset channel for $N = 1024$.

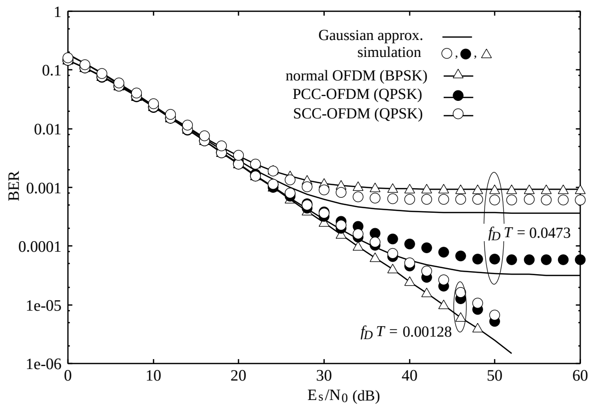

Figure 4. The average BER comparison between the normal OFDM, PCC-OFDM, and SCC-OFDM over the multipath fading channel with $N = 128$.

approximation to SCC-OFDM may be used for DCT-OFDM up to $f_O T = 0.07$.

In Fig. 4, we compare the average BERs calculated from the SINR approximation and the approximation (I-5) and those obtained by simulation over the four-path Rayleigh fading channel assumed in Fig. 1. In this simulation, we let $N = 128$ and $f_D T = 0.00128$, 0.0473, for which the SINR approximation is almost exact. QPSK is assumed for th PCC-OFDM and SCC-OFDM while BPSK is assumed for the normal OFDM to make data rate the same. The approximations and simulation results match well for the normal OFDM while, for the PCC-OFDM and SCC-OFDM, there are small gaps between them at a large SNR.

From these preliminary results, we may conclude that the SINR approximations are almost exact for $f_D T$ and $f_O T$ less than 0.1 and are useful to estimate the expected BER.

E. Nyquist windowing

We consider a symmetric Nyquist window of roll-off ρ and window length N in Fig. I-1. Windowing may be applied at the transmitter as well as at the receiver. However, we analyze the performance of windowing at the receiver only as in [1] and [2]. Only numerical results are given for windowing at both transmitter and receiver.

1) Windowing at the receiver: In the first part, it is shown that

$$\begin{aligned} A^{\mathrm{W}}(n) &\triangleq \frac{1}{N}\sum_{k=0}^{N-1}\sum_{\ell=0}^{L-1} g_k h_{k,\ell} e^{j\frac{-2\pi\ell n}{N_{\mathrm{S}}}} \\ W^{\mathrm{W}}(n) &\triangleq \frac{1}{N}\sum_{k=0}^{N-1} g_k w_k e^{-j\frac{2\pi k n}{N_{\mathrm{S}}}} \\ I^{\mathrm{W}}(n) &\triangleq \frac{1}{N}\sum_{\substack{m=0\\ m\neq n}}^{N_{\mathrm{S}}-1} a_m \sum_{k=0}^{N-1}\sum_{\ell=0}^{L-1} g_k h_{k,\ell} e^{j\frac{2\pi\ell m}{N_{\mathrm{S}}}} \\ &\qquad \times e^{-j\frac{2\pi k(n-m)}{N_{\mathrm{S}}}} \end{aligned}$$

Thus, it is not difficult to see that the power of the respective terms are given as

$$\mathrm{E}\left[|A^{\mathrm{W}}(n)|^2\right] = \frac{1}{N^2}\sum_{k=0}^{N-1}\sum_{k'=0}^{N-1}\alpha_{k-k'} g_k g_{k'}, \quad (15)$$

$$\mathrm{E}\left[|W^{\mathrm{W}}(n)|^2\right] = \frac{N_o}{N}\sum_{k=0}^{N-1} g_k^2, \quad (16)$$

$$\begin{aligned} \mathrm{E}\left[|I^{\mathrm{W}}(n)|^2\right] &= \frac{N_{\mathrm{S}}E_{\mathrm{s}}'}{N^2}\sum_{k=0}^{N-1} g_k^2 + \frac{2N_{\mathrm{S}}E_{\mathrm{s}}'\Re[\alpha_{N_{\mathrm{S}}}]}{N^2} \\ &\quad \times \sum_{k=0}^{N_{\mathrm{S}}-1} g_k g_{k+N_{\mathrm{S}}} - E_{\mathrm{s}}'\mathrm{E}\left[|A^{\mathrm{W}}(n)|^2\right] \\ &= \frac{N_{\mathrm{S}}^2 E_{\mathrm{s}}'\Re[\alpha_{N_{\mathrm{S}}}]}{N^2} + \frac{N_{\mathrm{S}}E_{\mathrm{s}}'(1-\Re[\alpha_{N_{\mathrm{S}}}])}{N^2} \\ &\quad \times \sum_{k=0}^{N-1} g_k^2 - E_{\mathrm{s}}'\mathrm{E}\left[|A^{\mathrm{W}}(n)|^2\right], \quad (17) \end{aligned}$$

where we used the identity (I-13) in the last equality.

2) Triangular windowing at the receiver: We first consider the performance of the triangular window

$$g_k = \begin{cases} \frac{2k}{N}, & 0 \le k < \frac{N}{2}, \\ \frac{2(N-k)}{N}, & \frac{N}{2} \le k < N, \end{cases}$$

with $\rho = 1$.

In Appendix II-.2, we show the following approximation.

$$\mathrm{E}\left[|A^{\mathrm{W,Tr}}(n)|^2\right] \approx \frac{1}{4}\left\{1 - \left(1 - \frac{4}{N^2}\right)\frac{\mathcal{S}_2}{24} + \frac{\mathcal{S}_4}{1280}\right\}. \quad (18)$$

Substituting the above approximation and the identity

$$\frac{1}{N}\sum_{k=0}^{N-1} g_k^2 = \frac{1}{3}\left(1 + \frac{2}{N^2}\right) \quad (19)$$

into (17) and applying the approximation (31) in Appendix I, we have

$$\mathrm{E}\left[|I^{\mathrm{W,Tr}}(n)|^2\right] \approx \frac{E_{\mathrm{s}}'\mathcal{S}_4}{24 \cdot 1920}.$$

The noise power (16) is, from (19), approximated by $\mathrm{E}\left[|W^{\mathrm{W}}(n)|^2\right] \approx \frac{N_o}{3}$.

Therefore, the SINR of the triangular-windowed OFDM is given by

$$\Gamma^{\mathrm{W,Tr}}(n) \approx \left\{ \frac{\mathcal{S}_4}{11520} + \frac{2}{3\bar{\gamma}} \right\}^{-1}, \qquad (20)$$

where we let $E_{\mathrm{s}}' = 2E_{\mathrm{s}}$ since the utilized subcarriers are halved. Compared to PCC and SCC, there are SNR loss of the factor of $\frac{3}{4}$.

3) Optimal windowing at the receiver: We next consider an optimal window and show that, for $\rho = 1$, the optimal window coincides with the triangular window at the limit of large SNRs.

We first consider an optimal window that minimize the noise and interference terms. Later, this window is shown to minimize the SINR, too. To make notations simple, we let $\mu = \frac{N}{N_{\mathrm{S}}}$.

From (16) and (17), the interference plus noise power is written as, for $0 \le n < N$,

$$\begin{aligned} &\mathrm{E}\left[|I^{\mathrm{W}}(n)|^2\right] + \mathrm{E}\left[|W^{\mathrm{W}}(n)|^2\right] \\ &= \frac{E_{\mathrm{s}}'\Re[\alpha_{N_{\mathrm{S}}}]}{\mu^2} + \left\{ N_o + \frac{E_{\mathrm{s}}'(1-\Re[\alpha_{N_{\mathrm{S}}}])}{\mu} \right\} \frac{1}{N} \sum_{k=0}^{N-1} g_k^2 \\ &\quad - E_{\mathrm{s}}' \mathrm{E}\left[|A^{\mathrm{W}}(n)|^2\right]. \end{aligned} \qquad (21)$$

The symmetric Nyquist window $\{g_k\}$ is determined if its shape is given for $0 \le k < \frac{\rho}{4}N$. Thus, we consider p_k, $0 \le k \le \frac{\rho}{4}N$, satisfying $p_{\frac{\rho}{4}N} = 0$, and represent a Nyquist window of length N as

$$g_k = \begin{cases} \frac{1}{2} - p_k, & 0 \le k < \frac{\rho}{4}N, \\ \frac{1}{2} + p_{\frac{\rho}{2}N-k}, & \frac{\rho}{4}N \le k < \frac{\rho}{2}N, \\ 1, & \frac{\rho}{2}N \le k < \left(1-\frac{\rho}{2}\right)N, \\ \frac{1}{2} + p_{k-(1-\frac{\rho}{2})N}, & \left(1-\frac{\rho}{2}\right)N \le k < \left(1-\frac{\rho}{4}\right)N, \\ \frac{1}{2} - p_{N-k}, & \left(1-\frac{\rho}{4}\right)N \le k < N. \end{cases} \qquad (22)$$

By direct calculation, then, we can show the following identity.

$$\frac{1}{N}\sum_{k=0}^{N-1} g_k^2 = \frac{1+(2-\mu)}{2\mu} - \frac{2p_0^2}{N} + \frac{4}{N}\sum_{k=0}^{\frac{\rho}{4}N} p_k^2. \qquad (23)$$

The next lemma, which is proved in Appendix III, gives an approximation of $\mathrm{E}\left[\left|A^{\mathrm{W}}(n)\right|^2\right]$.

Lemma 1: The following approximation holds.

$$\begin{aligned} \mathrm{E}\left[\left|A^{\mathrm{W}}(n)\right|^2\right] \approx\ & \frac{1}{\mu^2} - \frac{\mathcal{S}_2}{12\mu^4}\left[\mu^2 - 2(2-\mu)(\mu-1)\right] \\ & + \frac{4\mathcal{S}_2(\mu-1)}{N_{\mathrm{S}}\mu^4} \sum_{k=0}^{\frac{\rho}{4}N} \left(\frac{1}{2} - \frac{k}{N-N_{\mathrm{S}}}\right) p_k \end{aligned}$$

Using the expression (23) with terms proportional to N_W^{-1} omitted and then applying Lemma 1 to (21), we can approximate the interference plus noise power as

$$\begin{aligned} &\mathrm{E}\left[|I^{\mathrm{W}}(n)|^2\right] + \mathrm{E}\left[|W^{\mathrm{W}}(n)|^2\right] \\ &\approx \frac{N_o(3-\mu)}{2\mu} + \frac{E_{\mathrm{s}}'\mathcal{S}_2\{1-3(\mu-1)(2-\mu)\}}{12\mu^4} \\ &\quad + \left(N_o + \frac{E_{\mathrm{s}}'\mathcal{S}_2}{2\mu^3}\right)\frac{4}{N_{\mathrm{S}}\mu}\sum_{k=0}^{\frac{\rho}{4}N} p_k^2 \\ &\quad - \frac{4E_{\mathrm{s}}'\mathcal{S}_2(\mu-1)}{N_{\mathrm{S}}\mu^4}\sum_{k=0}^{\frac{\rho}{4}N}\left(\frac{1}{2} - \frac{k}{N-N_{\mathrm{S}}}\right)p_k \\ &= \frac{N_o(3-\mu)}{2\mu} + \frac{E_{\mathrm{s}}'\mathcal{S}_2\{1-3(\mu-1)(2-\mu)\}}{12\mu^4} \\ &\quad + \left(N_o + \frac{E_{\mathrm{s}}'\mathcal{S}_2}{2\mu^3}\right)\frac{4}{N_{\mathrm{S}}\mu}\sum_{k=0}^{\frac{\rho}{4}N} \tilde{p}_k^2 \\ &\quad - \frac{4E_{\mathrm{s}}'\mathcal{S}_2(\mu-1)}{N_{\mathrm{S}}\mu^4}\sum_{k=0}^{\frac{\rho}{4}N}\frac{k\tilde{p}_k}{N-N_{\mathrm{S}}} \end{aligned} \qquad (24)$$

where we let $\tilde{p}_k = p_{\frac{\rho}{4}N-k}$. Then, after some calculations, we have

$$\begin{aligned} &\mathrm{E}\left[|I^{\mathrm{W}}(n)|^2\right] + \mathrm{E}\left[|W^{\mathrm{W}}(n)|^2\right] \\ &\approx \frac{2\mu^3 N_o + E_{\mathrm{s}}'\mathcal{S}_2}{(\mu^4 N_{\mathrm{S}}/2)} \sum_{k=0}^{\frac{\rho}{4}N}\left(\tilde{p}_k - \frac{E_{\mathrm{s}}'\mathcal{S}_2}{2\mu^3 N_o + E_{\mathrm{s}}'\mathcal{S}_2}\cdot\frac{k}{N_{\mathrm{S}}}\right)^2 \\ &\quad + \frac{E_{\mathrm{s}}'\mathcal{S}_2}{12\mu^4}\left\{1 - 3(\mu-1)(2-\mu) - \frac{(\mu-1)^3 E_{\mathrm{s}}'\mathcal{S}_2}{2\mu^3 N_o + E_{\mathrm{s}}'\mathcal{S}_2}\right\} \\ &\quad + \frac{N_o(3-\mu)}{2\mu} \end{aligned}$$

Thus, the interference plus noise power is minimized for

$$\tilde{p}_k = \frac{E_{\mathrm{s}}'\mathcal{S}_2}{2\mu^3 N_o + E_{\mathrm{s}}'\mathcal{S}_2}\cdot\frac{k}{N_{\mathrm{S}}}$$

for $0 \le k \le \frac{\rho}{4}$.

Now, let $E_{\mathrm{s}}' = \mu E_{\mathrm{s}}$. Then, we have the optimal Nyquist window

$$g_k = \begin{cases} \dfrac{\mu^2 + \bar{\gamma}\mathcal{S}_2\left(1 - \frac{\mu}{2} + \frac{k}{N_{\mathrm{S}}}\right)}{2\mu^2 + \bar{\gamma}\mathcal{S}_2}, & 0 \le k < \frac{\rho}{2}N \\ 1, & \frac{\rho}{2}N \le k < \left(1-\frac{\rho}{2}\right)N \\ \dfrac{\mu^2 + \bar{\gamma}\mathcal{S}_2\left(1 + \frac{\mu}{2} - \frac{k}{N_{\mathrm{S}}}\right)}{2\mu^2 + \bar{\gamma}\mathcal{S}_2}, & \left(1-\frac{\rho}{2}\right)N \le k < N \end{cases}$$

and the associated SINR

$$\begin{aligned} \Gamma_{\min}^{\mathrm{W}}(n) \approx \Bigg[& \frac{\mathcal{S}_2}{12\mu^2}\left\{1 - 3(\mu-1)(2-\mu) - \frac{(\mu-1)^3\bar{\gamma}\mathcal{S}_2}{2\mu^2 + \bar{\gamma}\mathcal{S}_2}\right\} \\ & + \frac{(3-\mu)}{2\bar{\gamma}}\Bigg]^{-1} \end{aligned} \qquad (25)$$

This expression coincides with (8) for the normal OFDM when $\rho = 0$ ($\mu = 1$) and it is not difficult to see that this expression approaches to the expression (20) for the triangular window when $\rho = 1$ ($\mu = 2$) and $\bar{\gamma}\mathcal{S}_2$ is very large, except for the term including $\mathcal{S}_4$.

Fig. 5 gives an example of the optimal window for $\bar{\gamma}\mathcal{S}_2 = 20$ and $\rho = \frac{2}{3}$. The optimal window show a

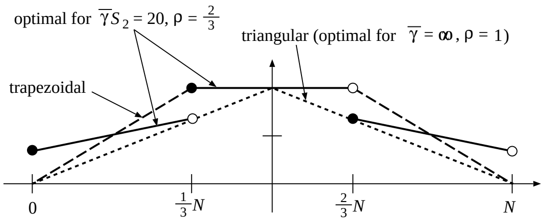

Figure 5. Optimal window for $\bar{\gamma}\mathcal{S}_2 = 20$ and $\rho = \frac{2}{3}$ (solid) and for $\bar{\gamma} = \infty$ and $\rho = 1$ (hatched)

quite similar behavior to the optimal window obtained in [10] for a channel only with a CFO. Since no closed form expression for the optimal solution is given in [10], however, we can not compare these solutions directly. In this respect, it is quite interesting to compare our solution with the Franks' double-jump spectrum [11] proposed for pulse waveform design under phase noise and timing jitter.

The triangular window and, as its generalization for $\rho < 1$, a trapezoidal window are considered in [2]. In Fig. 6, we compare the theoretical performance of the optimal window and the trapezoidal (triangular) window. For $\rho = 1$, although the triangular window is optimal only when $\rho = 1$ and $\bar{\gamma} = \infty$, the cost of using the triangular window for a finite $\bar{\gamma}$ is only several dBs for a small SNR. On the other hand, the cost of using the trapezoidal window for $\rho = \frac{2}{3}$ increases for a large SNR, as seen in the figure.

We can show, for $\rho = 1$ and for a large SNR, that the SINR of the optimal window is approximately given as

$$\Gamma^{\mathrm{W}} \approx \left\{ \frac{\mathcal{S}_4}{11520} + \frac{2}{3\bar{\gamma}} \cdot \frac{6 + \bar{\gamma}\mathcal{S}_2}{8 + \bar{\gamma}\mathcal{S}_2} \right\}^{-1}. \tag{26}$$

The term that includes $\mathcal{S}_2$ is immediately obtained from (25) for $\mu = 2$. We note, however, that the term that includes $\mathcal{S}_4$ may not be minimal for a finite $\bar{\gamma}$ since we did not consider $\mathcal{S}_4$ in the derivation of the optimal window. Derivation of (26) is tedious and hence omitted.

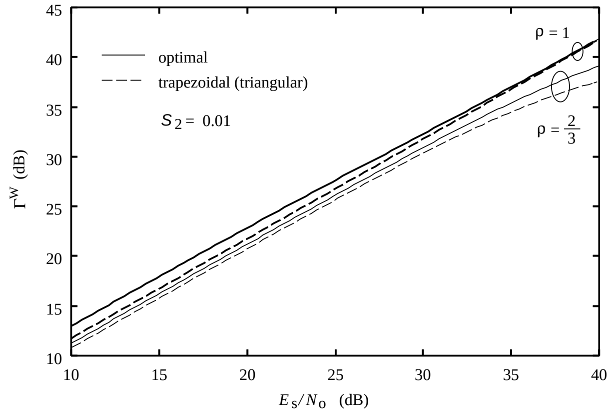

Figure 6. Comparison of the optimal and trapezoidal (triangular) windows

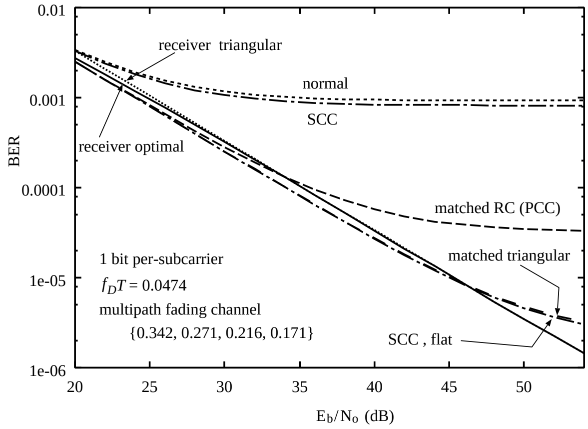

Figure 7. BER comparison of PCC, SCC, receiver windowing, and matched windowing

4) Matched windowing: From the expressions (I-17)-(I-19), it is straightforward to give expressions for $\mathrm{E}\left[|A^{\mathrm{MW}}(n)|^2\right]$, $\mathrm{E}\left[|I^{\mathrm{MW}}(n)|^2\right]$, and $\mathrm{E}\left[|W^{\mathrm{MW}}(n)|^2\right]$. For $L > 1$, however, approximations are not considered since these expressions are complex and since matched windowing schemes are not preferable because of their high PAPR.

F. Comparison

In Fig. 7, we compare the BERs of the normal OFDM, PCC-OFDM, SCC-OFDM with subtraction combining, and windowing of $\rho = 1$, respectively, calculated based on Gaussian approximation. We again considered a four-path fading channel with exponential PDP $\{0.342, 0.271, 0.216, 0.171\}$ and a flat fading channel. The flat fading channel is considered only for SCC-OFDM. The number of subcarriers is $N = 128$ and the normalized Doppler frequency $f_D T$ is 0.0474, which corresponds to the situation where the carrier frequency is 2 GHz, OFDM sampling period is $T_s = 1$ μsec, and the terminal speed is 200 Km/h. To fix the transmission rate to one bit per-subcarrier, we assume BPSK for the normal OFDM and QPSK for all other schemes. CFO is not considered.

Matched windowing schemes (including PCC) and SCC schemes show performances which depend on the considered channel. In Fig. 7, SCC with subtraction combining shows a drastic performance degradation when the channel becomes frequency-selective. The performance degradation of PCC due to the frequency-selectivity of the channel is not observable in this figure, but it exists as we will see next. The receiver windowing considered in this figure includes triangular windowing and optimal windowing. Both receiver windowing schemes show the best performance for a sufficiently large SNR. However, receiver windowing yields SNR loss which is seen at relatively small SNRs. The performance the optimal window is close to the matched windowing schemes for SNRs below 20 dB and to the receiver triangular windowing for SNRs above 30 dB. We can calculate the SINR bound of the triangular window at a high SNR from (20) and it is

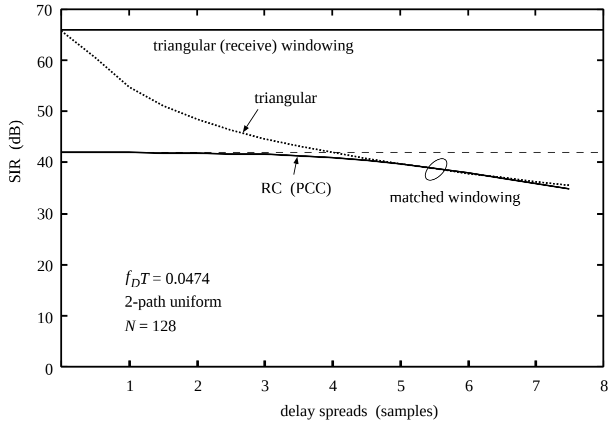

Figure 8. SIR comparison of PCC, receiver windowing, and matched windowing

about 59.9 dB for this case. Thus, its BER floor does not appear clearly in the figure.

Channel dependency of the performance of matched windowing is shown in Fig. 8, where the theoretical SIR is shown as a function of RMS delay spread for a two-path fading channel consisting of equal power paths. Two window functions, triangular and RC, are considered for matched windowing. The RC matched windowing, which is nothing but PCC, shows almost constant, but relatively small, SIRs for delay spreads below three, while the triangular matched windowing has SIR which is high at a small delay spread but decreases rapidly as the delay spread increase. For delay spreads above four, both schemes show similar behavior. This figure also shows that our SIR approximation for PCC, or the assumption (9), is not adequate for a large delay spread. The performance dependency on delay spread may becomes a problem in applying PCC to broadcasting such as digital TV [10], since sometimes quite a large delay spread is observed [13].

According to the above results, receiver windowing may be the best if the receiver can work in a high SNR situation, while matched windowing may be preferable if the receiver works in a SNR-limited situation and if the transmitter has a good linear amplifier. The complementary cumulative distribution function (CCDF) of PCC-OFDM shown in Fig. I-2, however, seems to discourage the use of PCC. SCC-OFDM with subtraction combining becomes totally inferior to windowing schemes including PCC-OFDM over a multipath fading channel and hence must be used optimal receiver discussed in the next section.

In the above BER comparisons, we only considered theoretical calculations based on Gaussian approximation. All the SINR approximations are quite close to the exact calculations for $f_D T = 0.0424$ and $N \geq 128$, as seen in the first part of this two-part paper, and, in the case of matched windowing including PCC, for delay spreads below three (samples). The accuracy of BER approximations is, however, generally dependent on whether the Doppler spread is dominant or the CFO as we have discussed at the end of Section I-II; Gaussian approximations match simulation results relatively well in most cases. Moreover, it also depends on whether the normal OFDM, PCC-OFDM, or SCC-OFDM are considered. However, since our aim is to compare different schemes, we only used theoretical calculations. Interested readers are consulted to see the previous references as well as [14], [15], and [16]. (See also [17].)

IV. BER ANALYSIS OF DIVERSITY SCHEMES

In this section, we consider two diversity schemes, SCC and CCC, and approximate their performances under the Gaussian ICI assumption. In the analysis, we assume that the receiver knows the channel completely.

A. SCC-OFDM with optimized combining

In the analysis of the performance of SCC-OFDM in conjunction with optimal detection, we restrict our attention to QPSK signals.

Let n be such that $0 \leq n < \frac{N}{2}$. Under the assumption that $\frac{E_s}{\hat{N}_o}$ is sufficiently large, we have derived an BER approximation (I-29), which is reproduced below.

$$P_b(n) \approx \frac{3}{4}\left|\frac{\hat{N}_o}{2E_s}\boldsymbol{H}_n^{-1}\boldsymbol{V}_n\right| \tag{27}$$

where, for

$$\boldsymbol{h}_n = \begin{bmatrix} \tilde{A}^S(n) \\ \tilde{A}^S(-1-n) \end{bmatrix} \text{ and } \boldsymbol{v}_n = \begin{bmatrix} \tilde{I}^S(n)+W_n \\ \tilde{I}^S(-1-n)+W_{N-1-n} \end{bmatrix},$$

we let

$$\boldsymbol{H}_n = \mathrm{E}\left[\boldsymbol{h}_n\boldsymbol{h}_n^H\right] \text{ and } \hat{N}_o\boldsymbol{V}_n = \mathrm{E}\left[\boldsymbol{v}_n\boldsymbol{v}_n^H\right].$$

We consider subcarriers which satisfy the condition,

$$\frac{1}{\left|N\sin\frac{\pi(2n+1)}{N}\right|} \ll 1 \quad \text{and} \quad \frac{1}{N^2\sin^2\frac{\pi(2n+1)}{N}} \approx 0. \tag{28}$$

The left-hand side of the condition is the order of 10^{-3} or less for $5 < n < \frac{N}{2} - 5$ and, hence, the condition holds almost the all subcarriers. Then, the following lemma is proved in Appendix III

Lemma 2: Under the assumption (3) and the condition (28), the following approximations hold, for $\xi = n$ and $-1-n$.

(a) $\mathrm{E}[|\tilde{A}^S(\xi)|^2] \approx \frac{1}{2}$

(b) $\mathrm{E}[\tilde{A}^S(n)\tilde{A}^{S*}(-1-n)] \approx -\frac{1}{2}P_{2n+1}$

(c) $\mathrm{E}[|\tilde{I}^S(\xi)|^2] \approx \frac{1}{12}E_s\mathcal{S}_2$

(d) $\mathrm{E}[\tilde{I}^S(n)\tilde{I}^{S*}(-1-n)] \approx \frac{1}{12}E_s P_{2n+1}\mathcal{S}_2$

From Lemma 2 we immediately have the approximations

$$\begin{aligned} \boldsymbol{H}_n &\approx \frac{1}{2}\begin{bmatrix} 1 & -P_{2n+1} \\ -P_{-(2n+1)} & 1 \end{bmatrix} \\ \hat{N}_o\boldsymbol{V}_n &\approx \frac{E_s\mathcal{S}_2}{12}\begin{bmatrix} 1 & P_{2n+1} \\ P_{-(2n+1)} & 1 \end{bmatrix} + N_o\begin{bmatrix} 1 & 0 \\ 0 & 1 \end{bmatrix} \end{aligned}$$

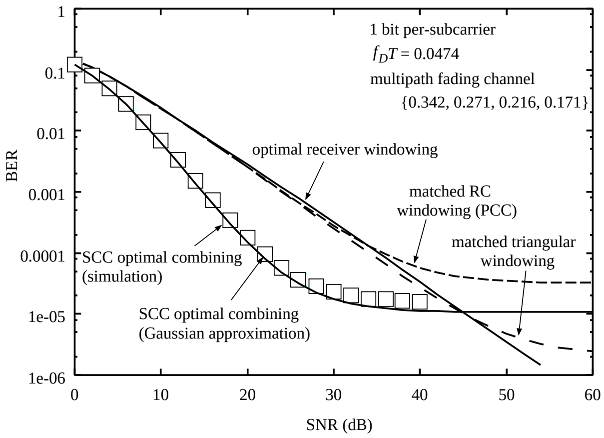

Figure 9. BER comparison of SCC with optimal combining, PCC, and windowing

Thus, from (27), we have an approximation

$$P_{\rm b}(n) \approx \frac{1}{192}\left\{\mathcal{S}_2+\frac{(12/\bar{\gamma})}{1+|P_{2n+1}|}\right\}\left\{\mathcal{S}_2+\frac{(12/\bar{\gamma})}{1-|P_{2n+1}|}\right\}$$

If $\mathcal{S}_2 \ll 1$, then the system shows the diversity order 2 as $P_{\rm b}(n) \approx (\bar{\gamma}^2[1-|P_{2n+1}|^2])^{-1}$ for low to moderate SNRs and has an error floor $P_{\rm b}(n) \approx \frac{\mathcal{S}_2^2}{192}$ for a sufficiently large SNR.

B. CCC-OFDM with optimized combining

We can obtain the approximate BER expression for CCC-OFDM by replacing $\tilde{A}^{\rm S}(\xi)$ and $\tilde{I}^{\rm S}(\xi)$ with $\tilde{A}^{\rm C}(\xi)$ and $\tilde{I}^{\rm C}(\xi)$, respectively and by applying the following lemma, whose proof is omitted since it is similar to and simpler than Lemma 2.

Lemma 3: We have, for $\xi = n$ and $n + \frac{N}{2}$,

(a) $\mathrm{E}[|\tilde{A}^{\rm C}(\xi)|^2] \approx \dfrac{1}{2}$

(b) $\mathrm{E}[\tilde{A}^{\rm C}(n)\tilde{A}^{\rm C*}\left(n+\frac{N}{2}\right)] \approx -\dfrac{1}{2}P_{\frac{N}{2}}$

(c) $\mathrm{E}[|\tilde{I}^{\rm C}(\xi)|^2] \approx \dfrac{1}{12}E_{\rm s}\mathcal{S}_2$

(d) $\mathrm{E}[\tilde{I}^{\rm C}(n)\tilde{I}^{\rm C*}\left(n+\frac{N}{2}\right)] \approx \dfrac{1}{12}E_{\rm s}P_{\frac{N}{2}}\mathcal{S}_2$

Then, for $0 \le n < \frac{N}{2}$, we have

$$P_{\rm b}(n) \approx \frac{1}{192}\left\{\mathcal{S}_2+\frac{(12/\bar{\gamma})}{1+|P_{\frac{N}{2}}|}\right\}\left\{\mathcal{S}_2+\frac{(12/\bar{\gamma})}{1-|P_{\frac{N}{2}}|}\right\} \quad (29)$$

where we let $E_{\rm s}' = \mathrm{E}\left[|a_n'|^2\right] = 2E_{\rm s}$.

C. BER comparison

In Fig 9, we show the results of the Gaussian approximation (27) and simulation for SCC-OFDM with optimized combining. Simulation was carried out for QAM modulation under the same condition as in Fig 7. Since the performance of SCC depends on subcarriers, simulation results and approximate calculations are averaged over subcarriers from $n = 5$ to $n = 54$. For Gaussian approximation, we assumed that the complex coefficients $\tilde{A}^{\rm S}(n)$ were known. The assumption is hardly true in practice and we used the time average $\bar{h}_\ell = \frac{1}{N}\sum_{k=0}^{N-1} h_{k,\ell}$, in stead of $h_{k,\ell}$, for computing $\tilde{A}^{\rm S}(n)$ in simulation.

Although the SCC-OFDM with optimal combining gives a slightly larger error floor than the matched windowing scheme, the effect of frequency diversity is apparent and show better performance than PCC-OFDM in this case. If we assume QPSK modulation, then, from (10), the BER floors of the PCC-OFDM and the SCC-OFDM with optimal combining are expected to be $\left(\frac{5}{48} - \frac{1}{\pi^2}\right)\cdot\frac{\mathcal{S}_2}{4}$ and $\frac{\mathcal{S}_2^2}{192}$, respectively, which shows that the SCC-OFDM with optimal combining has a smaller BER floor than PCC for $\mathcal{S}_2$ smaller than about 0.136, a large value. Thus, we can conclude that PCC is almost always inferior to SCC with optimal combining.

CCC-OFDM shows performance slightly better than SCC-OFDM since BERs are uniform over all subcarriers in CCC. However, its simulation result is omitted.

We note, as discussed in the first part of this two-part paper, the expressions for SCC-OFDM may be immediately applied to DCT-OFDM [9] with a suboptimal receiver where ICI is treated as noise. Only necessary modification is to replace T in our expressions with $2T$ since the inter-subcarrier space of DCT-OFDM is halved. The relationship of our performance expression for CCC-OFDM to the performance of (CR)V-OFDM [18][19] is not clear but interesting.

V. Conclusion

We have discussed SINR and BER performances of PCC, SCC, and windowing for uncoded OFDM systems over multipath channels with Doppler spreads and frequency offsets and given some asymptotic expressions for SINR and BER when Doppler spreads and frequency offsets are small, based on the Gaussian approximation. We also discussed certain optimality of triangular window and its extension. These results suggests that windowing is useful if frequency diversity effects are not considered because diversity is attained with some other mechanisms. If diversity effects is also considered for ICI suppression, on the other hand, our result suggests that SCC may be useful since it dose not increase PAPR much. It is rather surprising that PCC is not recommended in both cases because of its high PAPR and poorer performance than windowing with the triangular window function.

Recently, in [20], PCC is employed for a multi-antenna OFDM system to suppress Doppler-induced ICI. According to our result, receiver windowing is expected to show a better result. Since the ICI mitigation schemes discussed in this two-part paper are simple and easy to apply, they are useful to make multi-antenna OFDM systems sufficiently robust against the CFO and Doppler spread in the channel.

We finally note that, over a multi-path fading channel, CCC is generally superior to SCC because of its (subcarrier) position-independence. In this respect, performance analysis of CRV-OFDM [19] over channels with the Doppler spread and CFO is interesting.

REFERENCES

[1] R. Song and S.-H. Leung, "A novel OFDM receiver with second order polynomial Nyquist window function," *IEEE Commun. Lett.*, vol. 9, pp. 391-393, May 2005.

[2] M.-X. Chang, "A novel algorithm of inter-subchannel interference self-cancellation for OFDM systems," *IEEE Trans. Wireless Commun.*, vol. 6, pp. 2881-2893, Aug. 2007.

[3] R. H. Clarke, "A statistical theory of mobile radio reception," *Bell System Tech. J.*, vol. 47, pp. 957-1000, Jul/Aug. 1968.

[4] W. C. Jakes, ed., *Microwave Mobile Communications.* IEEE and John Wiley & Sons, Inc., 1974.

[5] R. Janaswamy, *Radiowave Propagation and Smart Antennas for Wireless Communications.* Kluwer Academic Publishers, 2001.

[6] J. R. Barry, E. A. Lee, and D. G. Messerschmitt, *Digital Communication*, 3rd ed., Kluwer Academic Pub., 2003.

[7] M. Russell and G. L. Stüber, "Interchannel interference analysis of OFDM in a mobile environment," in *Proc. IEEE 45th Veh. Tech. Conf. (VTC'95)*, July 1995, vol. 2, pp. 820-824.

[8] Y. (Geoffrey) Li and L. J. Cimini, Jr., "Bounds on the interchannel interference of OFDM in time-varying impairments," *IEEE Trans. Commun.*, vol. 49, pp. 401-404, Mar. 2001.

[9] P. Tan and N. C. Beaulieu, "A comparison of DCT-based OFDM and DFT-based OFDM in frequency offset and fading channels," *IEEE Trans. Commun.*, vol. 54, pp. 2113-2125, Nov. 2006.

[10] S. H. Muller-Weinfurt, "Optimum Nyquist windowing in OFDM receivers," *IEEE Trans. Commun.*, vol. 49, pp. 417-420, Mar. 2001.

[11] L. E. Franks, "Further results on Nyquist's problem in pulse transmission," *IEEE Trans. Commun. Tech.*, vol. COM-16, pp. 337-340, Apr. 1968.

[12] S. Lu and N. Al-Dhahir, "Coherent and differential ICI cancellation for mobile OFDM with application to DVB-H," *IEEE Trans. Wireless Commun.*, vol. 7, pp. 4110-4116, Nov. 2008.

[13] S. O'Leary, *Understanding Digital Terrestrial Broadcasting.* Artech House, 2000.

[14] A. S. Alaraimi and T. Hashimoto, "Performance analysis of polynomial cancellation coding for OFDM systems over time-varying Rayleigh fading channels," *IEICE Trans. Commun.*, vol. E88-B, pp. 471-477, Feb. 2005.

[15] A. S. Alaraimi and T. Hashimoto, "Analysis of coherent and non-coherent symmetric cancellation coding for OFDM over a multi-path Rayleigh fading channel," in *Proc. 64th IEEE Veh. Tech. Conf. (VTC'06)*, Sept. 2006.

[16] A. S. Alaraimi and T. Hashimoto, "Analysis of symmetric cancellation coding for OFDM over a multi-path Rayleigh fading channel," *IEICE Trans. Fundamentals*, vol. E90-A, pp. 1956-1964, Sept. 2007.

[17] A. S. Alaraimi, "Study on Self-interference-cancellation schemes for OFDM systems over channels with Doppler spread and frequency offset," Doctoral Dissertation, Univ. Elect.-Commun., 2007.

[18] X.-G. Xia, "Precoded and vector OFDM systems robust to channel spectral nulls and with reduced cyclic prefix length in single transmit antenna systems," *IEEE Trans. Commun.*, vol. 49, pp. 1363-1374, Aug. 2001.

[19] C. Han, T. Hashimoto, and N. Suehiro, "Constellation-rotated vector OFDM and its performance analysis over Rayleigh fading channels," *IEEE Trans. Communications*, vol. 58, pp. 828-838, March 2010.

[20] K. Kim, H. Park, and H. M. Kwon, "Rate-compatible SFBC-OFDM under rapidly time-varying channels," *IEEE Trans. Commun.*, vol. 59, pp. 2070-2077, Aug. 2011.

Takeshi Hashimoto received the B. E. M. E., and D. E degrees from Osaka University, respectively, in 1975, 1977, and 1981. He is currently a professor of the Department of Communication Engineering and Informatics, the Graduate School of Informatics and Engineering, the University of Electro-Communications, Japan. His research interests include information theory and communication theory.

Abdullah Saleh Alaraimi received the B. E. degree from Sultan Qaboos University, Oman in 1991 and received M. E. and D. E. degrees from University of Electro-Communications, Japan in, respectively, 2001 and 2007. From 1991 to 1999, he was an electronic engineer at Oman TV, Oman.

He is now with the Ministry of Information, Oman. His research interests are in broadcasting and wireless mobile communications systems.

Chenggao Han received the B. S. degree in Electronic Engineering from Tsinghua University, P. R. of China in 2000 and received M. E. and D. E. degrees from University of Tsukuba, Japan.

He is currently with the Graduate School of Informatics and Engineering, the University of Electro-Communications, Japan. His research interests are mobile communication systems, sequence design, and information theory.

APPENDIX I
CLARKE'S SPECTRUM AND RELATED APPROXIMATIONS

Under the WSSUS assumption, the power spectrum density (PSD) of the fading process $h(t)$ with maximum Doppler frequency $\omega_D \triangleq 2\pi f_D$ (rad/sec) is given by [3], [4], [5],

$$\int_{-\infty}^{\infty} J_0(\omega_D t) e^{-j\omega t}\, dt = \begin{cases} \frac{2}{\sqrt{\omega_D^2-\omega^2}}, & \text{for } |\omega| < \omega_D, \\ 0, & \text{otherwise,} \end{cases}$$

Then, the sampled fading process $h_k = h(T_s k)$, sampled each $T_s = T/N$, has the PSD, for $\omega \in (-\pi, \pi)$,

$$\sum_{k=-\infty}^{\infty} J_o(\omega_D T_s k) e^{-j\omega k} = \begin{cases} \frac{2}{\sqrt{(\omega_D T_s)^2-\omega^2}}, & |\omega| < \omega_D T_s, \\ 0, & \text{otherwise} \end{cases}$$

For $\omega_O \triangleq 2\pi f_O$ (rad/sec), we let

$$\alpha_k = \mathrm{E}\left[h_k h_0^*\right] = e^{j\omega_O T_s k} J_0(\omega_D T_s k)$$

then the PSD of h_k is , for $\omega \in (-\pi, \pi)$,

$$\mathcal{A}(\omega) = \begin{cases} \frac{2}{\sqrt{(\omega_D T_s)^2-(\omega-\omega_O T_s)^2}}, & |\omega - \omega_O T_s| < \omega_D T_s, \\ 0, & \text{otherwise} \end{cases}$$

provided that $\pi \geq \omega_D T_s + \omega_O T_s$. For notational convenience, we let $\mathcal{A}_N(\omega) \triangleq \frac{1}{N}\mathcal{A}\left(\frac{\omega}{N}\right)$

Since $e^{jx} \approx 1 + jx - \frac{x^2}{2} - j\frac{x^3}{6} + \frac{x^4}{24}$, the inverse Fourier transform of $\mathcal{A}_N(\omega)$ gives the following approximation, in terms of the spectrum moments (2),

$$\begin{aligned} \alpha_k & \\ &= \frac{1}{2\pi}\int e^{j\frac{\omega k}{N}}\mathcal{A}_N(\omega)\,d\omega \\ &\approx 1 + j\mathcal{S}_1\frac{k}{N} - \frac{\mathcal{S}_2}{2}\left(\frac{k}{N}\right)^2 - j\frac{\mathcal{S}_3}{6}\left(\frac{k}{N}\right)^3 + \frac{\mathcal{S}_4}{24}\left(\frac{k}{N}\right)^4 \quad (30) \end{aligned}$$

and

$$\alpha_{\frac{N}{2}} \approx 1 + j\frac{\mathcal{S}_1}{2} - \frac{\mathcal{S}_2}{8} - j\frac{\mathcal{S}_3}{48} + \frac{\mathcal{S}_4}{384} \quad (31)$$

Under the assumption (3), the following lemmas are proved in Appendix IV.

Lemma A1: For an integer m which is not zero nor a multiple of N, the following approximations hold,

(a) $F_{0,0} \approx 1 - \left(1 - \frac{1}{N^2}\right)\frac{\mathcal{S}_2}{12} + \frac{\mathcal{S}_4}{360}$

(b) $$F_{m,0} \approx -\frac{e^{j\frac{\pi m}{N}}\mathcal{S}_1}{2N\sin\frac{\pi m}{N}} - \frac{e^{j\frac{\pi m}{N}}\mathcal{S}_2\cos\frac{\pi m}{N}}{4N^2\sin^2\frac{\pi m}{N}} + \left(1 - \frac{3}{N^2\sin^2\frac{\pi m}{N}}\right)\frac{e^{j\frac{\pi m}{N}}\mathcal{S}_3}{24N\sin\frac{\pi m}{N}}$$

(c) $F_{m,\tilde{m}} \approx \frac{e^{j\frac{\pi(m-\tilde{m})}{N}}\mathcal{S}_2}{4N^2\sin\frac{\pi m}{N}\sin\frac{\pi\tilde{m}}{N}}$, for $\tilde{m} = \pm m$.

Lemma A2: The following approximations hold.

(a) $F_0 \approx \left(1 - \frac{1}{N}\right) - \left(1 - \frac{3}{N}\right)\frac{\mathcal{S}_2}{6} + \frac{\mathcal{S}_4}{120}$

(b) For an integer m which is not zero nor a multiple of N,
$$F_m \approx (-1)^{m+1}\left\{\frac{1}{N} + \frac{\mathcal{S}_1\cos\frac{\pi m}{N}}{N\sin\frac{\pi m}{N}} + \frac{\mathcal{S}_2}{N^2\sin^2\frac{\pi m}{N}} - \frac{\mathcal{S}_2}{2N}\right\}$$

APPENDIX II
SOME CALCULATIONS

1) Derivation of (13) in Section III-C: From Lemma A1, we have the following approximation, for $\xi = \frac{\pi(2n+1)}{N}$.

$$\begin{aligned} &\frac{\mathcal{S}_2}{2N^2\sin^2\xi} - \frac{1}{2}\Re\left[F_{2n+1,-(2n+1)} + F_{2n+1,2n+1} - 2F_{2n+1,0} - 2F_{-(2n+1),0}\right] \\ &\approx \frac{\mathcal{S}_2}{8N^2\sin^2\xi}\left\{3 + \cos 2\xi - 4\cos^2\xi\right\} \\ &= \frac{\mathcal{S}_2}{4N^2} \end{aligned}$$

2) Derivation of (18): The Fourier transform of the triangular window g_k is calculated as

$$\sum_{k=0}^{N-1} g_k e^{-j\omega k} = \frac{2}{N}e^{-j\omega\frac{N}{2}}\left(\frac{\sin\frac{\omega N}{4}}{\sin\frac{\omega}{2}}\right)^2.$$

Thus, from (15), we have

$$\mathrm{E}\left[|A^{\mathrm{W,Tr}}(n)|^2\right] = \frac{1}{8\pi}\int\left(\frac{\sin\frac{\omega}{4}}{\frac{N}{2}\sin\frac{\omega/4}{N/2}}\right)^4\mathcal{A}_N(\omega)\,d\omega$$

Then, employing an approximation

$$\left(\frac{\sin\frac{\omega}{4}}{\frac{N}{2}\sin\frac{\omega/4}{N/2}}\right)^4 \approx 1 - \left(1 - \frac{4}{N^2}\right)\frac{\omega^2}{24} + \frac{\omega^4}{5\cdot 256},$$

we have the desired approximation.

APPENDIX III
PROOF OF LEMMAS

1) Proof of Lemma 1: To simplify notations, let us introduce subsets

$$\begin{aligned} \mathcal{K}_1 &= \{k:\ 0 \le k < \tfrac{\rho}{4}N\} \\ \mathcal{K}_2 &= \{k:\ \tfrac{\rho}{4}N \le k < \tfrac{\rho}{2}N\} \\ \mathcal{K}_3 &= \{k:\ \tfrac{\rho}{2}N \le k < (1-\tfrac{\rho}{2})N\} \\ \mathcal{K}_4 &= \{k:\ (1-\tfrac{\rho}{2})N \le k < (1-\tfrac{\rho}{4})N\} \\ \mathcal{K}_5 &= \{k:\ (1-\tfrac{\rho}{4})N \le k < N\} \end{aligned}$$

and let $\mathcal{K} = \bigcup_{i=1}^{5}\mathcal{K}_i$. Then, if we introduce a new function as

$$q_k = \begin{cases} -p_k, & \text{for } k \in \mathcal{K}_1 \\ p_{\frac{\rho}{2}N-k}, & \text{for } k \in \mathcal{K}_2 \\ \frac{1}{2}, & \text{for } k \in \mathcal{K}_3 \\ p_{k-(1-\frac{\rho}{2})N}, & \text{for } k \in \mathcal{K}_4 \\ -p_{N-k}, & \text{for } k \in \mathcal{K}_5 \end{cases}$$

then $g_k = \frac{1}{2} + q_k$ for all k and, from (15), we have

$$\begin{aligned} &\mathrm{E}\left[\left|A^{\mathrm{W}}(n)\right|^2\right] \\ &= \frac{1}{N^2}\sum_{\mathcal{K}}\sum_{\mathcal{K}'}\alpha_{k-k'}\left(\frac{1}{2} + q_k\right)\left(\frac{1}{2} + q_k'\right) \quad (32) \end{aligned}$$

In this proof, we employ the convention that $\sum_{k\in\mathcal{K}_i} = \sum_{\mathcal{K}_i}$, $\sum_{k'\in\mathcal{K}_i} = \sum_{\mathcal{K}_i'}$, and $\mathcal{K}/\mathcal{K}_i = \bigcup_{j\ne i}\mathcal{K}_j$.

The double summation in (32) is expanded as

$$\begin{aligned} &\sum_{\mathcal{K}}\sum_{\mathcal{K}'}\alpha_{k-k'}\left(\frac{1}{2} + q_k\right)\left(\frac{1}{2} + q_k'\right) \\ &= \frac{1}{4}\sum_{\mathcal{K}}\sum_{\mathcal{K}'}\alpha_{k-k'} + \frac{1}{2}\sum_{\mathcal{K}}\sum_{\mathcal{K}'}\alpha_{k-k'}q_{k'} \\ &\quad + \frac{1}{2}\sum_{\mathcal{K}}\sum_{\mathcal{K}'}\alpha_{k-k'}q_k + \sum_{\mathcal{K}}\sum_{\mathcal{K}'}\alpha_{k-k'}q_k q_{k'} \quad (33) \end{aligned}$$

Since $q_k = \frac{1}{2}$ for $k \in \mathcal{K}_3$, the right-hand side is further expanded as follows.

$$
\begin{aligned}
&\frac{1}{4}\sum_{\mathcal{K}}\sum_{\mathcal{K}'}\alpha_{k-k'}+\frac{1}{4}\sum_{\mathcal{K}}\sum_{\mathcal{K}'_3}\alpha_{k-k'}\\
&+\frac{1}{4}\sum_{\mathcal{K}_3}\sum_{\mathcal{K}'}\alpha_{k-k'}+\frac{1}{4}\sum_{\mathcal{K}_3}\sum_{\mathcal{K}'_3}\alpha_{k-k'}\\
&+\frac{1}{2}\sum_{\mathcal{K}}\sum_{\mathcal{K}'/\mathcal{K}'_3}\alpha_{k-k'}q_{k'}+\frac{1}{2}\sum_{\mathcal{K}/\mathcal{K}_3}\sum_{\mathcal{K}'}\alpha_{k-k'}q_k\\
&+\frac{1}{2}\sum_{\mathcal{K}_3}\sum_{\mathcal{K}'/\mathcal{K}'_3}\alpha_{k-k'}q_{k'}+\frac{1}{2}\sum_{\mathcal{K}/\mathcal{K}_3}\sum_{\mathcal{K}'_3}\alpha_{k-k'}q_k\\
&+\sum_{\mathcal{K}/\mathcal{K}_3}\sum_{\mathcal{K}'/\mathcal{K}'_3}\alpha_{k-k'}q_kq_{k'}
\end{aligned}
\tag{34}
$$

We note that all the imaginary parts of α_k eventually vanish after summation and hence that we can consider α_k as real-valued and approximate as $\alpha_k \approx 1-\frac{\mathcal{S}_2}{2}\left(\frac{k}{N}\right)^2$. Then, the constant parts, the parts independent of q_k, of (34) are given, after straightforward but elaborate calculation, as

$$
\begin{aligned}
&\frac{N^2}{4}-\frac{\mathcal{S}_2N^2(N^2-1)}{8N^2\cdot 6}\\
&+\frac{N(2N_{\mathrm{S}}-N)}{4}-\frac{\mathcal{S}_2(2N_{\mathrm{S}}-N)(N^2-2NN_{\mathrm{S}}+2N_{\mathrm{S}}^2-1)}{8N\cdot 6}\\
&+\frac{N(2N_{\mathrm{S}}-N)}{4}-\frac{\mathcal{S}_2(2N_{\mathrm{S}}-N)(N^2-2NN_{\mathrm{S}}+2N_{\mathrm{S}}^2-1)}{8N\cdot 6}\\
&+\frac{(2N_{\mathrm{S}}-N)^2}{4}-\frac{\mathcal{S}_2(2N_{\mathrm{S}}-N)^2(N^2-4N_{\mathrm{S}}N+4N_{\mathrm{S}}^2-1)}{8N^2\cdot 6}\\
&= N_{\mathrm{S}}^2-\frac{\mathcal{S}_2N_{\mathrm{S}}^2}{12N^2}\left\{N^2-2(2N_{\mathrm{S}}-N)(N-N_{\mathrm{S}})-1\right\}
\end{aligned}
\tag{35}
$$

The first order parts, the parts including either q_k or $q_{k'}$, of (34) are given as

$$
\begin{aligned}
&\sum_{\mathcal{K}}\sum_{\mathcal{K}'_1}\frac{p_{k'}}{2}\left(-\alpha_{k-k'}+\alpha_{k+k'-N+N_{\mathrm{S}}}+\alpha_{k-k'-N_{\mathrm{S}}}-\alpha_{k+k'-N}\right)\\
&+\sum_{\mathcal{K}_1}\sum_{\mathcal{K}'}\frac{p_k}{2}\left(-\alpha_{k-k'}+\alpha_{-k-k'+N-N_{\mathrm{S}}}+\alpha_{k-k'+N_{\mathrm{S}}}-\alpha_{-k-k'+N}\right)\\
&+\sum_{\mathcal{K}_3}\sum_{\mathcal{K}'_1}\frac{p_{k'}}{2}\left(-\alpha_{k-k'}+\alpha_{k+k'-N+N_{\mathrm{S}}}+\alpha_{k-k'-N_{\mathrm{S}}}-\alpha_{k+k'-N}\right)\\
&+\sum_{\mathcal{K}_1}\sum_{\mathcal{K}'_3}\frac{p_k}{2}\left(-\alpha_{k-k'}+\alpha_{-k-k'+N-N_{\mathrm{S}}}+\alpha_{k-k'+N_{\mathrm{S}}}-\alpha_{-k-k'+N}\right)\\
&\approx \frac{1}{2}\sum_{\mathcal{K}}\sum_{\mathcal{K}'_1}\frac{\mathcal{S}_2}{2N^2}(-2k'-2N_{\mathrm{S}}+2N)p_{k'}\\
&\quad+\frac{1}{2}\sum_{\mathcal{K}_1}\sum_{\mathcal{K}'}\frac{\mathcal{S}_2}{2N^2}(-2k-2N_{\mathrm{S}}+2N)p_k\\
&\quad+\frac{1}{2}\sum_{\mathcal{K}_3}\sum_{\mathcal{K}'_1}\frac{\mathcal{S}_2}{2N^2}(-2k'-2N_{\mathrm{S}}+2N)p_{k'}\\
&\quad+\frac{1}{2}\sum_{\mathcal{K}_1}\sum_{\mathcal{K}'_3}\frac{\mathcal{S}_2}{2N^2}(-2k-2N_{\mathrm{S}}+2N)p_k\\
&= 4\mathcal{S}_2(N-N_{\mathrm{S}})\left(\frac{N_{\mathrm{S}}}{N}\right)^2\sum_{k=0}^{\frac{\rho}{4}}\left(\frac{1}{2}-\frac{k}{N-N_{\mathrm{S}}}\right)p_k
\end{aligned}
\tag{36}
$$

Finally, the second order parts, the parts including both q_k and $q_{k'}$ of (34) are calculated as

$$
\begin{aligned}
&\sum_{\mathcal{K}_1}\sum_{\mathcal{K}'_1}\left\{\alpha_{k-k'}-\alpha_{k+k'-N+N_{\mathrm{S}}}-\alpha_{k-k'-N_{\mathrm{S}}}+\alpha_{k+k'-N}\right.\\
&-\alpha_{-k-k'+N-N_{\mathrm{S}}}+\alpha_{-k+k'}+\alpha_{-k-k'+N-2N_{\mathrm{S}}}-\alpha_{-k+k'-N_{\mathrm{S}}}\\
&-\alpha_{k-k'+N_{\mathrm{S}}}+\alpha_{k+k'-N+2N_{\mathrm{S}}}+\alpha_{k-k'}-\alpha_{k+k'-N+N_{\mathrm{S}}}\\
&\left.+\alpha_{-k-k'+N}-\alpha_{-k+k'+N_{\mathrm{S}}}-\alpha_{-k-k'+N-N_{\mathrm{S}}}+\alpha_{-k+k'}\right\}p_kp_{k'}
\end{aligned}
\tag{37}
$$

Substituting the approximation $\alpha_k = 1-\frac{\mathcal{S}_2}{8}\left(\frac{k}{N_{\mathrm{S}}}\right)^2$ for the α_k's in the above expression, it is not difficult to see that the summation of terms within "{ }" vanishes for each k and each k' and hence the above summation itself does.

Substituting the expressions (35) and (36) into (34) and considering the conclusion for (37), we obtain an approximation of (32). This proves the lemma. ■

2) Proof of Lemma 2: The expectations $\mathrm{E}[|\tilde{A}^{\mathrm{S}}(n)|^2]$ and $\mathrm{E}[\tilde{A}^{\mathrm{S}}(n)\tilde{A}^{\mathrm{S}*}(-1-n)]$ are calculated and approximated, with the use of Lemma A1 in Appendix I, as follows.

$$
\begin{aligned}
&\mathrm{E}\left[|\tilde{A}^{\mathrm{S}}(n)|^2\right]\\
&= \frac{1}{2}\sum_{\ell=0}^{L-1}\frac{p_\ell}{N^2}\sum_{k=0}^{N-1}\sum_{k'=0}^{N-1}\alpha_{k-k'}\\
&\qquad\times\left\{1-e^{-j\frac{2\pi(2n+1)k}{N}}e^{j\frac{2\pi(2n+1)\ell}{N}}\right\}\\
&\qquad\times\left\{1-e^{j\frac{2\pi(2n+1)k'}{N}}e^{-j\frac{2\pi(2n+1)\ell}{N}}\right\}\\
&= \frac{1}{2}F_{0,0}+\frac{1}{2}F_{2n+1,2n+1}-\Re\left[P_{-(2n+1)}F_{2n+1,0}\right]\\
&\approx \frac{1}{2}-\frac{\mathcal{S}_2}{24}+\frac{\Re[e^{j\frac{\pi(2n+1)}{N}}P_{-(2n+1)}]\mathcal{S}_1}{2N\sin\frac{\pi(2n+1)}{N}}
\end{aligned}
$$

where we used the fact that $F_{2n+1,2n+1}$ is negligible from the assumptions (3) and (28). The same result is obtained for $\mathrm{E}[|\tilde{A}^{\mathrm{S}}(-1-n)|^2]$. This proves the statement (a).

On the other hand, we have

$$
\begin{aligned}
&\mathrm{E}\left[\tilde{A}^{\mathrm{S}}(n)\tilde{A}^{\mathrm{S}*}(-1-n)\right]\\
&= -\frac{1}{2}\sum_{\ell=0}^{L-1}\frac{p_\ell}{N^2}\sum_{k=0}^{N-1}\sum_{k'=0}^{N-1}\alpha_{k-k'}e^{-j\frac{2\pi(2n+1)\ell}{N}}\\
&\qquad\times\left\{1-e^{-j\frac{2\pi(2n+1)k}{N}}e^{j\frac{2\pi(2n+1)\ell}{N}}\right\}\\
&\qquad\times\left\{1-e^{-j\frac{2\pi(2n+1)k'}{N}}e^{j\frac{2\pi(2n+1)\ell}{N}}\right\}\\
&= -\frac{1}{2}P_{2n+1}F_{0,0}-\frac{1}{2}P_{-(2n+1)}F_{2n+1,-(2n+1)}\\
&\qquad+\frac{1}{2}F_{2n+1,0}+\frac{1}{2}F_{0,-(2n+1)}\\
&\approx -\frac{1}{2}P_{2n+1}\left(1-\frac{\mathcal{S}_2}{12}\right).
\end{aligned}
\tag{38}
$$

This proves the statement (b).

For the proof of the remaining statements, we introduce some definitions.

$$\hat{\alpha}_{2k} \triangleq \begin{cases} \alpha_{2k-N}, & \text{for } k>0, \\ 1, & \text{for } k=0, \\ \alpha_{2k+N}, & \text{for } k<0, \end{cases}$$

$$D^{(1)}_{2n+1} \triangleq \sum_{\ell=0}^{L-1} p_\ell \frac{1}{N} \sum_{k=-\ell}^{\ell} [\alpha_{2k} - \hat{\alpha}_{2k}] e^{-j\frac{2\pi(2n+1)k}{N}}$$

$$D^{(2)}_{2n+1} \triangleq \sum_{\ell=0}^{L-1} p_\ell e^{-j\frac{2\pi(2n+1)\ell}{N}} \frac{1}{N} \sum_{k=-\ell}^{\ell} [\alpha_{2k} - \hat{\alpha}_{2k}]$$

The following lemma is proved later.

Lemma C3: For a sufficiently small $f_D T$ and for sufficiently large N, we have approximations

(a) $$D^{(1)}_{2n+1} \approx \frac{\mathcal{S}_1 \Re\left[e^{-j\frac{\pi(2n+1)}{N}}(1-P_{2n+1})\right]}{N\sin\frac{\pi(2n+1)}{N}} + \frac{\mathcal{S}_2 \Im\left[e^{-j\frac{\pi(2n+1)}{N}}(1-P_{2n+1})\right]}{2N\sin\frac{\pi(2n+1)}{N}}$$

(b) $$D^{(2)}_{2n+1} \approx \frac{P^{(2)}_{2n+1}\mathcal{S}_2}{N}$$

where $P^{(2)}_m$ is the Fourier transform of $p^{(2)}_\ell = \ell p_\ell$.

We note

$$\mathrm{E}\left[|\tilde{I}^{\mathrm{S}}(n)|^2\right] = \sum_{m=0}^{\frac{N}{2}-1} \mathrm{E}\left[|A_{m,n} - A_{-1-m,n}|^2\right] - \mathrm{E}[|\tilde{A}^{\mathrm{S}}(n)|^2]$$

The first term in the right-hand side is calculated as follows.

$$\begin{aligned}
&\sum_{m=0}^{\frac{N}{2}-1} \mathrm{E}\left[|A_{m,n} - A_{-1-m,n}|^2\right] \\
&= \sum_{\ell=0}^{L-1} \frac{p_\ell}{N^2} \sum_{k=0}^{N-1}\sum_{k'=0}^{N-1} \alpha_{k-k'} \times \left\{ N\delta_{k-k'} - N\delta_{[k+k'-2\ell]_N} e^{-j\frac{2\pi(2n+1)(k-\ell)}{N}} \right\} \\
&= 1 - \sum_{\ell=0}^{L-1} \frac{p_\ell}{N} \left\{ \sum_{k=0}^{2\ell} \alpha_{2[k-\ell]} e^{-j\frac{2\pi(2n+1)(k-\ell)}{N}} + \sum_{k=2\ell+1}^{N-1} \alpha_{2[k-\ell]-N} e^{-j\frac{2\pi(2n+1)(k-\ell)}{N}} \right\} \\
&= 1 - \sum_{\ell=0}^{L-1} \frac{p_\ell}{N} \left\{ \sum_{k=-\ell}^{\ell} [\alpha_{2k} - \hat{\alpha}_{2k}] e^{-j\frac{2\pi(2n+1)k}{N}} + 1 - \sum_{k=1-\frac{N}{2}}^{\frac{N}{2}-1} \alpha_{2k} e^{-j\frac{2\pi(2n+1)k}{N}} \right\} \\
&= 1 - D^{(1)}_{2n+1} + \left(F_{2n+1} - \frac{1}{N}\right)
\end{aligned}$$

Therefore, we have

$$\begin{aligned}
\mathrm{E}\left[|\tilde{I}^{\mathrm{S}}(n)|^2\right] &\approx 1 - D^{(1)}_{2n+1} + \left(F_{2n+1} - \frac{1}{N}\right) - 1 + \frac{\mathcal{S}_2}{12} - \frac{\Re[e^{j\frac{\pi(2n+1)}{N}} P_{-(2n+1)}]\mathcal{S}_1}{N\sin\frac{\pi(2n+1)}{N}} \\
&\approx \frac{\mathcal{S}_2}{12}
\end{aligned}$$

The same is true for $\mathrm{E}[|\tilde{I}^{\mathrm{S}}(-1-n)|^2]$ and this proves the statement (c).

Finally, we note

$$\begin{aligned}
&\mathrm{E}\left[\tilde{I}^{\mathrm{S}}(n)\tilde{I}^{\mathrm{S}*}(-1-n)\right] \\
&= E_{\mathrm{s}} \sum_{m=0}^{\frac{N}{2}-1} \mathrm{E}\left[(A_{m,n} - A_{-1-m,n})(A_{m,-1-n} - A_{-1-m,-1-n})^*\right] \\
&\quad - E_{\mathrm{s}}\mathrm{E}\left[A^{\mathrm{S}}(n)A^{\mathrm{S}*}(-1-n)\right]
\end{aligned}$$

The first term of the right-hand side is rewritten as

$$\begin{aligned}
&\sum_{m=0}^{\frac{N}{2}-1} \mathrm{E}\left[(A_{m,n} - A_{-1-m,n})(A_{m,-1-n} - A_{-1-m,-1-n})^*\right] \\
&= -\sum_{m=0}^{\frac{N}{2}-1}\sum_{\ell=0}^{L-1} \frac{p_\ell}{N^2} \sum_{k=0}^{N-1}\sum_{k'=0}^{N-1} \alpha_{k-k'} \\
&\quad \times \Bigg\{ \left(e^{j\frac{2\pi m(k-k')}{N}} + e^{-j\frac{2\pi(m+1)(k-k')}{N}}\right) e^{-j\frac{2\pi(nk+[n+1]k')}{N}} \\
&\qquad - \left(e^{-j\frac{2\pi m(k+k'-2\ell)}{N}} + e^{j\frac{2\pi(m+1)(k+k'-2\ell)}{N}}\right) \\
&\qquad \times e^{j\frac{2\pi\ell}{N}} e^{-j\frac{2\pi(n+1)(k+k')}{N}} \Bigg\} \\
&= \sum_{\ell=0}^{L-1} \frac{p_\ell}{N} \sum_{k=0}^{N-1}\sum_{k'=0}^{N-1} \alpha_{k-k'}\delta_{k-k'} e^{-j\frac{2\pi[(2n+1)k]}{N}} \\
&\quad - \sum_{\ell=0}^{L-1} \frac{p_\ell}{N} \sum_{k=0}^{N-1}\sum_{k'=0}^{N-1} \alpha_{k-k'}\delta_{[k+k'-2\ell]_N} e^{-j\frac{2\pi(2n+1)\ell}{N}}
\end{aligned}$$

The first term in the right-hand side is zero since $2n+1$ is not a multiple of N and the second term is enumerated both for $k+k'=2\ell$ and for $k+k'=2\ell+N$ as follows.

$$\begin{aligned}
&= -\sum_{\ell=0}^{L-1} \frac{p_\ell}{N} e^{-j\frac{2\pi(2n+1)\ell}{N}} \left\{ \sum_{k=0}^{2\ell} \alpha_{2[k-\ell]} + \sum_{k=2\ell+1}^{N-1} \alpha_{2[k-\ell]-N} \right\} \\
&= -\sum_{\ell=0}^{L-1} \frac{p_\ell}{N} e^{-j\frac{2\pi(2n+1)\ell}{N}} \left\{ \sum_{k=-\ell}^{\ell} \alpha_{2k} + \sum_{k=1-\frac{N}{2}+\ell}^{\frac{N}{2}-1-\ell} \alpha_{2k} \right\} \\
&= -\sum_{\ell=0}^{L-1} \frac{p_\ell}{N} e^{-j\frac{2\pi(2n+1)\ell}{N}} \left\{ \sum_{k=-\ell}^{\ell} [\alpha_{2k} - \hat{\alpha}_{2k}] + \sum_{k=1-\frac{N}{2}}^{\frac{N}{2}-1} \alpha_{2k} + 1 \right\} \\
&= -D^{(2)}_{2n+1} - P_{2n+1}\left(F_0 + \frac{1}{N}\right)
\end{aligned}$$

Thus, together with (38) and Lemma C3, we have

$$\begin{aligned}
&\mathrm{E}\left[\tilde{I}^{\mathrm{S}}(n)\tilde{I}^{\mathrm{S}*}(-1-n)\right] \\
&\approx -D^{(2)}_{2n+1} + P_{2n+1}\left(F_{0,0} - F_0 - \frac{1}{N}\right) \\
&\approx \frac{P_{2n+1}\mathcal{S}_2}{12}.
\end{aligned}$$

This gives the statement (d) and completes the proof. ■

3) Proof of Lemma C3: From the definition $\hat{\alpha}_k$, we know $\alpha_{2k} - \hat{\alpha}_{2k} = 0$ for $k = 0$ and, from the approximation (30) in Appendix I, we have an approximation

$$\alpha_{2k} - \hat{\alpha}_{2k} \approx \begin{cases} j\mathcal{S}_1 + \frac{\mathcal{S}_2}{2}\left(1 - \frac{4k}{N}\right), & \text{for } 0 < k, \\ -j\mathcal{S}_1 + \frac{\mathcal{S}_2}{2}\left(1 + \frac{4k}{N}\right), & \text{for } k < 0 \end{cases}$$

Thus, for $\frac{4L}{N} \ll 1$, we have

$$\begin{aligned} D_{2n+1}^{(1)} &\approx \frac{2\mathcal{S}_1}{N}\Im\left[\sum_{\ell=1}^{L-1} p_\ell \sum_{k=1}^{\ell} e^{j\frac{2\pi(2n+1)k}{N}}\right] \\ &\quad + \frac{\mathcal{S}_2}{N}\Re\left[\sum_{\ell=1}^{L-1} p_\ell \sum_{k=1}^{\ell} e^{j\frac{2\pi(2n+1)k}{N}}\right] \\ &= \frac{\mathcal{S}_1\Re\left[e^{-j\frac{\pi(2n+1)}{N}}(1-P_{2n+1})\right]}{N\sin\frac{\pi(2n+1)}{N}} \\ &\quad + \frac{\mathcal{S}_2\Im\left[e^{-j\frac{\pi(2n+1)}{N}}(1-P_{2n+1})\right]}{2N\sin\frac{\pi(2n+1)}{N}} \end{aligned}$$

On the other hand, the approximation to $D_{2n+1}^{(2)}$ follows from

$$\begin{aligned} D_{2n+1}^{(2)} &= \sum_{\ell=0}^{L-1} p_\ell e^{-j\frac{2\pi(2n+1)\ell}{N}} \frac{1}{N}\sum_{k=-\ell}^{\ell} \Re[\alpha_{2k} - \hat{\alpha}_{2k}] \\ &\approx \frac{\mathcal{S}_2}{N}\sum_{\ell=0}^{L-1} \ell p_\ell e^{-j\frac{2\pi(2n+1)\ell}{N}} \end{aligned}$$

This completes the proof of the lemma. ■

APPENDIX IV
PROOF OF MAIN LEMMAS

1) Proof of Lemma A1: For $\theta = \frac{2\pi m}{N}$, we first note

$$\begin{aligned} F_{m,m} &= \frac{1}{N^2}\sum_{k=0}^{N-1}\sum_{k'=0}^{N-1} \alpha_{k-k'} e^{j\frac{2\pi m(k-k')}{N}} \\ &= \frac{1}{2\pi}\int \left|\frac{1}{N}\sum_{k=0}^{N-1} e^{-j(\theta-\omega)k}\right|^2 \mathcal{A}(\omega)\, d\omega \\ &= \frac{1}{2\pi}\int \left(\frac{\sin\left[\frac{\theta N}{2} - \frac{\omega}{2}\right]}{N\sin\left[\frac{\theta}{2} - \frac{\omega}{2N}\right]}\right)^2 \mathcal{A}_N(\omega)\, d\omega. \end{aligned}$$

Now, we let $m = 0$. Then, from the approximation $\sin x \approx x - \frac{1}{6}x^3 + \frac{1}{120}x^5$ for a sufficiently small x, we have $(\frac{\sin[\omega/2]}{N\sin[\omega/2N]})^2 \approx 1 - \left(1 - \frac{1}{N^2}\right)\frac{\omega^2}{12} + \frac{\omega^4}{360}$. Thus, we have

$$F_{0,0} \approx 1 - \left(1 - \frac{1}{N^2}\right)\frac{\mathcal{S}_2}{12} + \frac{\mathcal{S}_4}{360}$$

This proves the statement (a).

We next consider that m is not zero nor a multiple of N. Then, the right-hand side of (39) is re-casted as

$$\frac{1}{2\pi}\int\left(\frac{\sin\frac{\omega}{2}}{N\sin\left[\frac{\theta}{2} - \frac{\omega}{2N}\right]}\right)^2 \mathcal{A}_N(\omega)\, d\omega$$

For $a = \sin\frac{\theta}{2}$ and $b = \cos\frac{\theta}{2}$, we have $(\frac{\sin[\omega/2]}{N\sin[\theta/2-\omega/(2N)]})^2 \approx \frac{\omega^2}{4(aN)^2} + \frac{b\omega^3}{4(aN)^3}$. Thus, we have an approximation

$$F_{m,m} \approx \frac{\mathcal{S}_2}{4(aN)^2} + \frac{b\mathcal{S}_3}{4(aN)^3}$$

This proves the statement (c) for $\tilde{m} = m$.

We next consider the case that $\tilde{m} = -m$. The following lemma is proved later.

Lemma D4: For m_1 and m_2 whose sum is not zero nor a multiple of N, the identity

$$\begin{aligned} &\sum_{k=0}^{N-1}\sum_{k'=0}^{N-1} \alpha_{k-k'} e^{-j\frac{2\pi(m_1k+m_2k')}{N}} \\ &= \frac{e^{j\frac{\pi(m_1+m_2)}{N}}}{\sin\frac{\pi(m_1+m_2)}{N}} \sum_{\xi=0}^{N-1} \Im\left[\alpha_\xi e^{-j\frac{2\pi m_1}{N}\xi} - \alpha_\xi e^{j\frac{2\pi m_2}{N}\xi}\right] \end{aligned}$$

hold.

For $\theta = \frac{2\pi m}{N}$, we have

$$\begin{aligned} &\Im\left[\sum_{\xi=0}^{N-1}\alpha_\xi e^{-j\theta\xi}\right] \\ &= \frac{1}{2\pi}\int_{-\pi}^{\pi}\Im\left[\sum_{\xi=0}^{N-1} e^{-j(\theta-\omega)\xi}\right]\mathcal{A}(\omega)\, d\omega \\ &= -\frac{1}{2\pi}\int \frac{\sin\left(\frac{\theta}{2} - \frac{\omega}{2N} + \frac{\omega}{2}\right)\sin\frac{\omega}{2}}{\sin\left(\frac{\theta}{2} - \frac{\omega}{2N}\right)} \cdot \mathcal{A}_N(\omega)\, d\omega \end{aligned}$$

where the first equality follows since $\mathcal{A}(j\omega)$ is real-valued and the last equality follows since $N\theta$ is an integral multiple of π.

Letting $a = \sin\frac{\theta}{2}$ and $b = \cos\frac{\theta}{2}$ and applying the approximation

$$\begin{aligned} &\frac{\sin\left(\frac{\pi m}{N} - \frac{\omega}{2N} + \frac{\omega}{2}\right)\sin\frac{\omega}{2}}{\sin\left(\frac{\pi m}{N} - \frac{\omega}{2N}\right)} \\ &= \frac{\cos\left(\frac{\pi m}{N} - \frac{\omega}{2N}\right)\sin^2\frac{\omega}{2}}{\sin\left(\frac{\pi m}{N} - \frac{\omega}{2N}\right)} + \cos\frac{\omega}{2}\sin\frac{\omega}{2} \\ &\approx \left\{\frac{b\omega^2}{4a} + \frac{\omega^3}{8a^2N} - \left(1 - \frac{3}{(aN)^2}\right)\frac{b\omega^4}{48a}\right\} + \left\{\frac{\omega}{2} - \frac{\omega^3}{12}\right\}, \end{aligned}$$

we have

$$\begin{aligned} &\frac{1}{N}\Im\left[\sum_{\xi=1}^{N-1}\alpha_\xi e^{-j\theta\xi}\right] \\ &\approx -\frac{\mathcal{S}_1}{2N} - \frac{b\mathcal{S}_2}{4aN} + \left(1 - \frac{3}{2a^2N}\right)\frac{\mathcal{S}_3}{12N} \\ &\quad + \left(1 - \frac{3}{(aN)^2}\right)\frac{b\mathcal{S}_4}{48aN} \end{aligned} \quad (39)$$

Thus, we have

$$\frac{1}{N}\sum_{\xi=1}^{N-1}\Im\left[\alpha_\xi e^{-j\theta\xi} - \alpha_\xi e^{j\theta\xi}\right] \approx -\frac{b\mathcal{S}_2}{2aN} + \frac{b\mathcal{S}_4}{24aN},$$

which, together with Lemma D4, proves the expression (c) for $\tilde{m} = -m$.

To prove the remaining statement, we note the following approximation obtained from (30) in Appendix I

$$\frac{1}{N}\Im\left[\sum_{\xi=1}^{N-1}\alpha_\xi\right] \approx \left(1-\frac{1}{N}\right)\frac{\mathcal{S}_1}{2}-\left(1-\frac{1}{N}\right)^2\frac{\mathcal{S}_3}{24}$$

Combining with (39), we have

$$\begin{aligned}&\frac{1}{N}\sum_{\xi=1}^{N-1}\Im\left[\alpha_\xi e^{-j\theta\xi}-\alpha_\xi\right]\\ &\approx -\frac{\mathcal{S}_1}{2}-\frac{b\mathcal{S}_2}{4aN}+\left(1-\frac{3}{(aN)^2}+\frac{1}{N^2}\right)\frac{\mathcal{S}_3}{24}+\frac{b\mathcal{S}_4}{48aN}.\end{aligned}$$

This approximation, together with Lemma D4, proves (b) and hence completes the proof. ■

2) Proof of Lemma A2: We note

$$\sum_{k=-\infty}^{\infty}\alpha_{2k}e^{-j\omega k}=\mathcal{A}_2(\omega)=\frac{N}{2}\mathcal{A}_N\left(\frac{N\omega}{2}\right)$$

and

$$\sum_{k=-(\frac{N}{2}-1)}^{\frac{N}{2}-1}e^{-j\omega k}=\frac{\sin[\omega(N-1)/2]}{\sin[\omega/2]}$$

Thus, for $\theta=\frac{2\pi m}{N}$, we have

$$F_m = \frac{1}{2\pi}\int\frac{\sin\left(\frac{\theta(N-1)}{2}-\omega[1-\frac{1}{N}]\right)}{N\sin\left(\frac{\theta}{2}-\frac{\omega}{N}\right)}\mathcal{A}_N(\omega)\,d\omega$$

We first suppose $m=0$. Then, the integrand is approximated as

$$\begin{aligned}&\frac{\sin\left(\omega-\frac{\omega}{N}\right)}{N\sin\frac{\omega}{N}}\\ &= \frac{\sin\omega\cdot\cos\frac{\omega}{N}}{N\sin\frac{\omega}{N}}-\frac{1}{N}\cos\omega\\ &\approx \left(1-\frac{1}{N}\right)-\left(1-\frac{3}{N}\right)\frac{\omega^2}{6}+\left(1-\frac{5}{N}\right)\frac{\omega^4}{120}\end{aligned}$$

Therefore, we have

$$F_0 \approx \left(1-\frac{1}{N}\right)-\left(1-\frac{3}{N}\right)\frac{\mathcal{S}_2}{6}+\left(1-\frac{5}{N}\right)\frac{\mathcal{S}_4}{120}$$

and this proves the statement (a).

Next, let $\theta=\frac{2\pi m}{N}$ and let $a=\sin\frac{\pi m}{N}$ and $b=\cos\frac{\pi m}{N}$. Then, we have

$$\begin{aligned}&\frac{\sin\left(\frac{\theta}{2}[N-1]-\omega\left[1-\frac{1}{N}\right]\right)}{N\sin\left(\frac{\theta}{2}-\frac{\omega}{N}\right)}\\ &= (-1)^{m+1}\frac{\sin\left(\frac{\theta}{2}+\omega-\frac{\omega}{N}\right)}{N\sin\left(\frac{\theta}{2}-\frac{\omega}{N}\right)}\\ &= (-1)^{m+1}\left\{\frac{\cos\left(\frac{\theta}{2}-\frac{\omega}{N}\right)\sin\omega}{N\sin\left(\frac{\theta}{2}-\frac{\omega}{N}\right)}+\frac{\cos\omega}{N}\right\}\\ &\approx (-1)^{m+1}\left\{\frac{1}{N}+\frac{b\omega}{aN}-\left(1-\frac{2}{a^2N}\right)\frac{\omega^2}{2N}\right\}\end{aligned}$$

Thus, we have

$$F_m\approx(-1)^{m+1}\left\{\frac{1}{N}+\frac{b\mathcal{S}_1}{aN}-\left(1-\frac{2}{a^2N}\right)\frac{\mathcal{S}_2}{2N}\right\}$$

This gives the statement (b) and complete the proof of the lemma. ■

3) Proof of Lemma D4: For $\theta_i=\frac{2\pi m_i}{N}$, $i=1,2$, we have the following equalities.

$$\begin{aligned}&\sum_{k=0}^{N-1}\sum_{k'=0}^{N-1}\alpha_{k-k'}e^{-j(\theta_1 k+\theta_2 k')}\\ &= \sum_{\xi=0}^{N-1}\alpha_\xi e^{-j\theta_1\xi}\sum_{k'=0}^{N-1-\xi}e^{-j(\theta_1+\theta_2)k'}\\ &\quad+\sum_{\xi=1-N}^{-1}\alpha_\xi e^{-j\theta_1\xi}\sum_{k'=-\xi}^{N-1}e^{-j(\theta_1+\theta_2)k'}\\ &= \sum_{\xi=0}^{N-1}\alpha_\xi e^{-j\theta_1\xi}\cdot\frac{1-e^{-j(\theta_1+\theta_2)(N-\xi)}}{1-e^{-j(\theta_1+\theta_2)}}\\ &\quad+\sum_{\xi=1-N}^{-1}\alpha_\xi e^{-j\theta_1\xi}\frac{e^{j(\theta_1+\theta_2)\xi}-e^{-j(\theta_1+\theta_2)N}}{1-e^{-j(\theta_1+\theta_2)}}\\ &= \sum_{\xi=1}^{N-1}\alpha_\xi e^{-j\theta_1\xi}\cdot\frac{1-e^{j(\theta_1+\theta_2)\xi}}{1-e^{-j(\theta_1+\theta_2)}}\\ &\quad+\sum_{\xi=1}^{N-1}\alpha_\xi^* e^{j\theta_1\xi}\frac{e^{-j(\theta_1+\theta_2)\xi}-1}{1-e^{-j(\theta_1+\theta_2)}}\\ &= \sum_{\xi=1}^{N-1}\frac{\alpha_\xi(e^{-j\theta_1\xi}-e^{j\theta_2\xi})+\alpha_\xi^*(e^{-j\theta_2\xi}-e^{j\theta_1\xi})}{1-e^{-j(\theta_1+\theta_2)}}\\ &= \frac{2j}{1-e^{-j(\theta_1+\theta_2)}}\sum_{\xi=0}^{N-1}\Im\left[\alpha_\xi e^{-j\theta_1\xi}-\alpha_\xi e^{j\theta_2\xi}\right]\end{aligned}$$

This completes the proof. ■